



Rapid Flow Cytometry-Based Assay for the Functional Classification of *MEFV* Variants

Yoshitaka Honda¹ · Yukako Maeda¹ · Kazushi Izawa¹ · Takeshi Shiba^{1,2} · Takayuki Tanaka^{1,3} · Haruna Nakaseko⁴ · Keisuke Nishimura⁵ · Hiroki Mukoyama⁶ · Masahiko Isa-Nishitani¹ · Takayuki Miyamoto¹ · Hiroshi Nihira¹ · Hirofumi Shibata¹ · Eitaro Hiejima¹ · Osamu Ohara⁷ · Junko Takita¹ · Takahiro Yasumi¹ · Ryuta Nishikomori⁸

Received: 23 October 2020 / Accepted: 9 March 2021 / Published online: 17 March 2021

© The Author(s), under exclusive licence to Springer Science+Business Media, LLC, part of Springer Nature 2021

Abstract

Purpose Pathogenic *MEFV* variants cause pyrin-associated autoinflammatory diseases (PAADs), which include familial Mediterranean fever (FMF), FMF-like disease, and pyrin-associated autoinflammation with neutrophilic dermatosis (PAAND). The diagnosis of PAADs is established by clinical phenotypic and genetic analyses. However, the pathogenicity of most *MEFV* variants remains controversial, as they have not been functionally evaluated. This study aimed to establish and validate a new functional assay to evaluate the pathogenicity of *MEFV* variants.

Methods We transfected THP-1 monocytes with 32 *MEFV* variants and analyzed their effects on cell death with or without stimulation with *Clostridium difficile* toxin A (TcdA) or UCN-01. These variants were classified using hierarchical cluster analysis. Macrophages were obtained from three healthy controls and two patients with a novel homozygous *MEFV*^{P257L} variant, for comparison of IL-1 β secretion using a cell-based assay and a novel THP-1-based assay.

Results Disease-associated *MEFV* variants induced variable degrees of spontaneous or TcdA/UCN-01-induced cell death in THP-1. Cell death was caspase-1 dependent and was accompanied by ASC speck formation and IL-1 β secretion, indicating that pathogenic *MEFV* variants induced abnormal pyrin inflammasome activation and subsequent pyroptotic cell deaths in this assay. The *MEFV* variants ($n = 32$) exhibiting distinct response signatures were classified into 6 clusters, which showed a good correlation with the clinical phenotypes. Regarding the pathogenicity of *MEFV*^{P257L} variants, the results were consistent between the cell-based assay and the THP-1-based assay.

Conclusion Our assay facilitates a rapid and comprehensive assessment of the pathogenicity of *MEFV* variants and contributes to a refined definition of PAAD subtypes.

Keywords Pyrin-associated autoinflammatory disease · classical FMF · PAAND · FMF-like disease · pyrin inflammasome · in vitro functional assay

Yoshitaka Honda and Yukako Maeda contributed equally to this work.

✉ Kazushi Izawa
kizawa@kuhp.kyoto-u.ac.jp

✉ Takahiro Yasumi
yasumi@kuhp.kyoto-u.ac.jp

¹ Department of Pediatrics, Faculty of Medicine, Kyoto University Graduate School of Medicine, 54 Kawahara-cho, Shogoin, Sakyo-ku, Kyoto 606-8507, Japan

² Department of Pediatrics, Tenri Hospital, Tenri, Japan

³ Department of Pediatrics, Otsu Red Cross Hospital, Otsu, Japan

⁴ Department of Infection and Immunology, Aichi Children's Health and Medical Center, Obu, Japan

⁵ Department of Endocrinology and Rheumatology, Kurashiki Central Hospital, Kurashiki, Japan

⁶ Department of Rheumatology and Clinical Immunology, Kyoto University Graduate School of Medicine, Kyoto, Japan

⁷ Kazusa DNA Research Institute, Kisarazu, Japan

⁸ Department of Pediatrics and Child Health, Kurume University School of Medicine, Kurume, Japan

Introduction

FMF is the most common hereditary systemic autoinflammatory disease (SAID) and is characterized by recurrent fever, polyserositis, arthritis, and a limited erythematous skin rash [1, 2]. Classically, FMF is diagnosed using clinical criteria [3]. However, this is challenging and time-consuming since clinical symptoms can vary between patients [4, 5].

In 1997, it was reported that the *MEFV* gene, which is composed of 10 exons and encodes pyrin, is associated with FMF [6, 7]. Since then, it has been shown that four founding variants in exon 10 (p.M680I, p.M694I, p.M694V, and p.V726A) account for almost 80% of clinically and ethnically typical FMF cases [8]. Moreover, extensive genetic testing for SAID has revealed an unexpected association between *MEFV* and other clinically distinct diseases, such as pyrin-associated autoinflammation with neutrophilic dermatosis (PAAND) [9, 10] and autosomal dominant FMF-like diseases [11–13], which are caused by mutations in exons 2, 3, 5, or 8. Consequently, the novel umbrella term, pyrin-associated autoinflammatory diseases (PAADs), has been proposed to define all diseases caused by *MEFV* mutations [14]. Therefore, genetic analysis has become important and indispensable for accurately diagnosing PAADs [15], although there is a lack of conclusive genetic evidence for around 30% of patients diagnosed with clinical FMF [16].

More than 370 *MEFV* variants have been recorded in Infevers, a website dedicated to mutations in hereditary autoinflammatory diseases [17]. However, the majority of the reported variants are categorized as “variants of unknown significance” (VOUS or VUS), partly due to a lack of reliable functional assays. Recent improvements in our understanding of the precise molecular mechanisms underlying the activation of pyrin inflammasomes [18–22] has led to the development of novel patient cell-based assays that utilize newly identified pyrin inflammasome activators, such as *Clostridium difficile* toxin A (TcdA) [23] or UCN-01 [22, 24]. However, the coexistence (either in *cis* or in *trans*) of variants in a single patient makes it difficult to evaluate the pathogenicity of individual *MEFV* variants.

Here, we show that disease-associated *MEFV* mutants induce varying degrees of spontaneous or rapid TcdA/UCN-01-induced cell death in human THP-1 monocytes, depending on the nature of the variant. Using hierarchical cluster analysis, these variants were categorized into six clusters, which correlated with the clinical phenotypes. The degree of cell death induction varied among the variants, which might correlate with the clinical impact of each variant. Therefore, our assay facilitates a rapid and comprehensive assessment of the pathogenicity of the *MEFV* variants and contributes to a refined definition of PAAD subtypes.

Methods

Patients and Healthy Control Subjects

Two patients with homozygous *MEFV*^{P2257L}, their healthy mother with heterozygous *MEFV*^{P2257L} variant, and 3 healthy controls with no *MEFV* variants were enrolled in this study. All the participants were Japanese. For detailed clinical course, see [Results](#) section.

All study participants provided informed consent, and the study design was approved by the ethics committee of Kyoto University Hospital (protocols G1091, G0729, G0457, G0432), and this study is conducted in compliance with the Declaration of Helsinki.

Cell Lines

THP-1 cells (TIB-202) were purchased from the American Type Culture Collection (Manassas, VA, US) and maintained in Roswell Park Memorial Institute (RPMI)-1640 medium (Sigma-Aldrich, St. Louis, MO, USA) supplemented with 10% fetal calf serum (Thermo Fisher Scientific, Waltham, MA, USA) and streptomycin/penicillin (Meiji, Tokyo, Japan).

Plasmids

C-terminal enhanced green fluorescent protein (eGFP)-fusion *MEFV* was introduced into pcDNA-5/TO (V103320, Sigma-Aldrich). Each *MEFV* variant was generated by PCR-based mutagenesis using KOD plus (Toyobo, Osaka, Japan) or HiFi DNA assembly (New England Biolabs, Ipswich, MA, USA). Primer sequences are shown in Table S1.

Nucleofection and Flow Cytometry

THP-1 cells (1×10^6) were transfected with 500 ng of plasmids encoding GFP-fused *MEFV* variants using Nucleofector device IIb and kit V (Lonza, Basel, Switzerland). Immediately after nucleofection, 10 ng/mL of phorbol 12-myristate 13-acetate (FUJIFILM Wako, Osaka, Japan) was added. Cells were treated with colchicine (1 μ M, Sigma-Aldrich) or MCC950 (1 or 10 μ M as indicated, Sigma-Aldrich) after 2 h of transfection as indicated. Three hours after nucleofection, cells were stimulated with 1 μ g/mL of TcdA (List Biological Laboratories, Campbell, CA, USA) or 10 μ M UCN-01 (Sigma-Aldrich) for 3 h, stained with 7-amino-actinomycin D (7-AAD; BD; Becton and Dickinson Bioscience, Franklin Lakes, NJ, USA) and/or anti-Annexin V-PE (BD) as indicated. Cells were analyzed using a FACSVerse flow cytometer (BD) and FlowJo software (BD). Cell death was calculated as the percentage of 7-AAD-positive cells among GFP-positive cells. Spontaneous cell death (%) was defined as percentage of cell death without stimulation. “UCN-01/TcdA-induced cell

death enhancement (%)” was defined as the increased percentage of cell death upon UCN-01 or TcdA stimulation over spontaneous cell death: (percentage of cell death upon UCN-01/TcdA stimulation) - (percentage of spontaneous cell death).

Cytokine Secretion from Patient Macrophages

Peripheral blood mononuclear cells (PBMCs) were isolated with Lymphoprep (Alere Technologies, Waltham, MA, USA). CD14⁺ monocytes were sorted magnetically from PBMCs by the autoMACS Pro Separator (Miltenyi Biotec, Bergisch Gladbach, Germany), according to the manufacturer’s instructions. To obtain monocyte-derived macrophages, monocytes were cultured in RPMI-1640 supplemented with 10% FCS and a 50-ng/mL macrophage-colony stimulating factor (M-CSF; R&D Systems, Minneapolis, MN, USA) for 7 days.

Macrophages were harvested with Accumax (Innovative Cell Technologies, San Diego, CA, USA) and seeded in 96-well plates at 5×10^4 cells/well in RPMI-1640 medium, supplemented with 10% FCS. Colchicine (100 ng/mL) was added, and cells were incubated for 30 min. After 2 h of priming with 1 μ g/mL LPS (InvivoGen, San Diego, CA, USA), 1- μ g/mL TcdA was added, and supernatants were collected 4 h later. The IL-1 β concentration was measured in technical duplicates or triplicates by using the Bio-Plex Pro Human Cytokine Assay (Bio-Rad Laboratories, Hercules, CA, USA).

Statistical Analysis

Data were analyzed using GraphPad Prism software with one-way analysis of variance (ANOVA) followed by Dunnett’s multiple comparison test (versus the WT as a control group) or unpaired *t* test. A *p* value less than 0.05 was considered as significant. Hierarchical cluster analysis was performed using Ward’s method in R, and the number of clustering is determined using NbClust package [25].

Results

GFP-Fused *MEFV*^{M694V} Overexpression Caused Spontaneous and TcdA/UCN-01-Induced Cell Death in THP-1 Monocytes

Previously, we reported that pathogenic *NLRP3* variants induced rapid cell death in human THP-1 monocytes after 2–3 h of nucleofection [26–28]. To determine if similar method could be used to evaluate the pathogenicity of each *MEFV* variant, we compared THP-1 cell death induction after introducing wild-type (WT) pyrin and the most common FMF-

associated pathogenic pyrin^{M694V} variant. After 3 h of nucleofection with full GFP-fused pyrin expression, pyrin^{M694V} induced pyroptotic cell death (7-AAD (+) and Annexin V (+)) in THP-1 cells compared to WT (Fig. 1a–c, S1a). Moreover, TcdA and UCN-01 treatment enhanced pyroptotic cell death in a time-dependent manner, and these were significantly higher in the cells transfected with *MEFV*^{M694V} compared to the cells transfected with *MEFV*^{WT} (Fig. 1b, c). Although UCN-01 is known to trigger apoptosis [22], cell death induction in this assay was specific for pyroptosis (Fig. S1). Therefore, we defined the “cell death (%)” as the percentage of 7-AAD(+) cells among the GFP(+) cells. “Spontaneous cell death (%)” indicates the percentage of cell death without any stimulation. Because spontaneous cell death levels differed between the variants, we defined “UCN-01/TcdA-induced cell death enhancement (%)” as the increased percentage of cell death upon UCN-01 or TcdA stimulation over spontaneous cell death: (percentage of cell death upon UCN-01/TcdA stimulation) - (percentage of spontaneous cell death) to clearly describe the pure additive effect of UCN-01/TcdA treatment (Fig. 1b, c).

Cell death induction was associated with IL-1 β secretion (Fig. S2) and ASC speck formation (Fig. S3) and prevented by caspase-1 knockout (Fig. 1d, S4). In addition, cell death induction was partially inhibited by colchicine, but not by MCC950, an NLRP3 specific inhibitor (Fig. S5). These results indicate that this assay reflects pyrin inflammasome activation and subsequent pyroptotic cell death caused by pathogenic *MEFV* variants. Since no significant cell death was observed in cells expressing the empty GFP vector (Fig. S6a), and endogenous pyrin expression was low (Fig. S6b), the effect of endogenous pyrin in THP-1 cells was almost negligible in this assay.

The Mode of Cell Death Induction Enables the Functional Classification of *MEFV* Variants

Next, we selected 32 reported *MEFV* variants [4, 13, 15, 29–37] and evaluated their pathogenicity. The pathogenic score/status as per Infevers and the classification, according to the new guideline [15], as well as other relevant information including the minor allele frequency per individual variant are shown in Table S2. Transfection efficacy was high and equivalent among the selected variants, as assessed using GFP fluorescence through flow cytometry (Fig. S7). These 32 variants exhibited distinct signatures of cell death (Fig. 2), and we categorized them using hierarchical cluster analysis. The optimal number of clusters were calculated using NbClust [25]. We chose 6 clusters, because these were in good accordance with the previous reports (Fig. 3a).

Cluster 1 included only M694del, which is sometimes associated with dominantly inherited FMF, with increased spontaneous, UCN-01-induced, and TcdA-induced cell death.

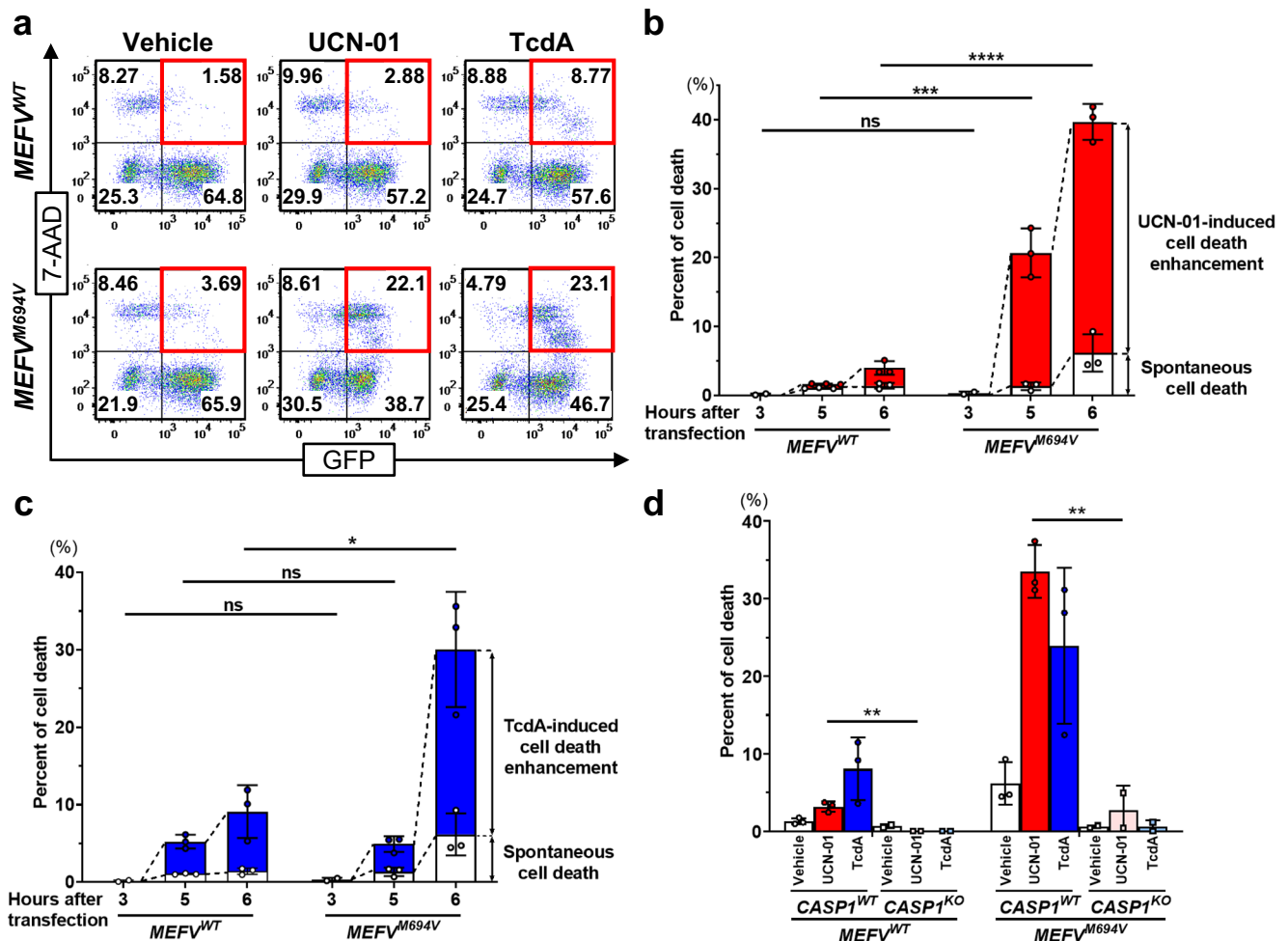


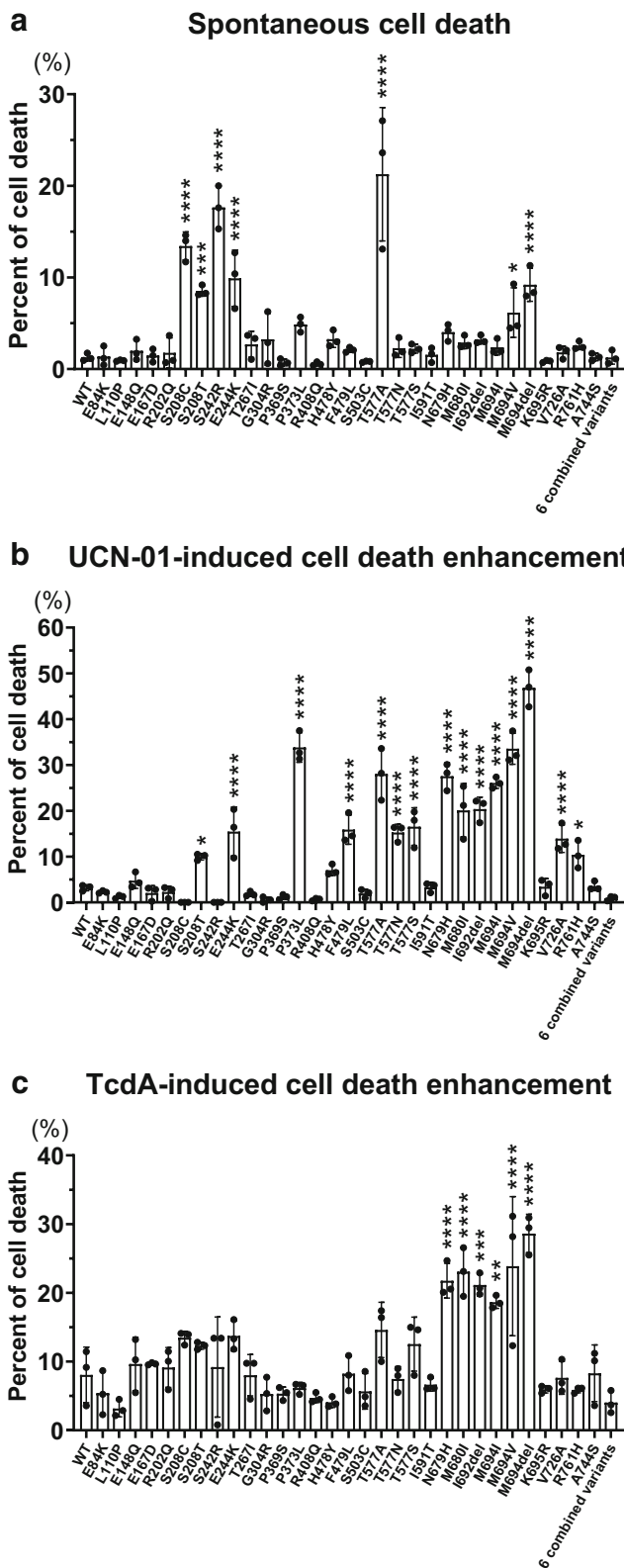
Fig. 1 GFP-fused *MEFV*^{M694V} induces spontaneous, TcdA/UCN-01-induced cell death in THP-1 monocytes. **a** Representative flow cytometry dot plots. *MEFV* expression was monitored by GFP fluorescence. The number in each quadrant indicates the percentage of cells. Cell death was measured as the percentage of 7-AAD-positive cells among GFP-positive cells (red rectangle). **b** Time course of spontaneous cell death (white) and UCN-01-induced cell death enhancement (red). **c** Time course of spontaneous cell death (white) and TcdA-induced cell death enhancement (blue). Cells were stimulated 3 h after transfection. Cell death was analyzed at the indicated time after transfection. Spontaneous cell death indicates cell death without stimulation. UCN-01/TcdA-induced cell death enhancement was calculated as cell death induced by each stimulant over

spontaneous cell death: [(percentage of cell death induced by UCN-01/TcdA stimulation) - (percentage of spontaneous cell death)]. If UCN-01/TcdA-induced cell death was a negative value, 0 was plotted. **d** Cell death was prevented by caspase-1 KO. Cells were stimulated 3 h after transfection and analyzed 6 h after transfection. Circle, *CASP1*^{WT} THP-1; rectangle, *CASP1*^{KO} THP-1. White/Gy, spontaneous cell death; red/pink, UCN-01-induced cell death enhancement; blue/light blue, TcdA-induced cell death enhancement. Data were analyzed by unpaired two-tailed *t* test. ns: nonsignificant, **p* < 0.05, ***p* < 0.01, ****p* < 0.001, *****p* < 0.0001. Data represent the mean ± standard deviation of three (b, c, and d (*CASP1*^{WT} THP-1)) or two (d (*CASP1*^{KO} THP-1)) independent experiments

Cluster 2 included exon 10 variants, including classical M680I, M694I, and M694V, as well as I692del and N679H. These variants were characterized by hyper-responsiveness to both TcdA and UCN-01. Cluster 3 was composed of two autosomal dominant FMF-like disease-associated variants, P373L and T577A. Cluster 4 contained FMF-associated variants (F479L, V726A, and R761H) and autosomal dominant FMF-like disease-associated variants (H478Y and T577S/N), as well as two 14-3-3 binding site-associated variants (S208T and E244K). The variants in clusters 3 and 4 showed enhanced responsiveness to UCN-01 but normal response to TcdA. Two other 14-3-3 binding site-associated variants,

S208C and S242R, were categorized in cluster 5 with increased spontaneous cell death, but with no obvious hyper-response to UCN-01 and TcdA. No significant increase in spontaneous cell death and TcdA/UCN-01-induced cell death enhancement were observed among the variants in cluster 6. In addition, the *MEFV*^{L110P-E148Q-R202Q-P369S-R408Q-S503} variant carrying six *cis* amino acid alterations induced levels of cell death similar to the WT, suggesting that these variants are unlikely to exert additive or synergistic effects in this experimental setting.

To determine the optimal cut-off value for our THP-1-based assay, we performed receiver operating characteristic



◀ **Fig. 2** Cell death induced by each *MEFV* variant with or without UCN-01/TcdA treatment. **a** Spontaneous cell death induced by each *MEFV* variant. Cell death enhancement after **b** UCN-01 or **c** TcdA stimulation. Cells were stimulated 3 h after transfection, and cell death was analyzed 6 h after transfection. “6 combined variants” denotes *MEFV*^{L110P-E148Q-R202Q-P369S-R408Q-S503}. If UCN-01/TcdA-induced cell death enhancement ((percentage of cell death induced by UCN-01/TcdA stimulation) - (percentage of spontaneous cell death)) was a negative value, 0 was plotted. Data were analyzed by one-way ANOVA followed by Dunnett’s multiple comparison test (versus the WT as a control group). ns: nonsignificant, **p* < 0.05, ***p* < 0.01, ****p* < 0.001, *****p* < 0.0001. Data represent the mean ± standard deviation of three independent experiments

1.755% for spontaneous cell death, 5.515% for UCN-01-induced cell death enhancement, and 11.62% for TcdA-induced cell death enhancement (Fig. 3e–g).

Homozygous *MEFV*^{P257L} Causes Autosomal Recessive FMF

We next examined if we could utilize our THP-1 based functional assay to evaluate the pathogenicity of the novel *MEFV*^{P257L} variant that we recently identified in two patients from one family in the homozygous state (Fig. 4a). There are no previous reports on the clinical phenotype of patients with homozygous *MEFV*^{P257L} variant. Patient 1 (III-1) was a 50-year-old man whose symptoms of recurrent fever, chest and abdominal pain, episcleritis, and arthralgia/arthritis developed at the age of five. To treat joint deformity, he underwent multiple arthroplasties: right ankle (at 12 years of age) and left metacarpophalangeal joints (at 14 years of age). In his childhood, he was diagnosed with suppurative arthritis or with bacterial infection such as that of *Streptococcus pyogenes* during each episode. He was diagnosed with oligoarticular juvenile idiopathic arthritis in his middle age, and the administration of methotrexate (from 48 years of age), iguratimod (from 49 years of age), colchicine, and etanercept, and anti-TNF-α recombinant antibody (from 49 years of age) was partially effective for the control of his symptoms. At the age of 50, he was given a suspected clinical diagnosis of autoinflammatory disease, and panel gene test for autoinflammatory diseases revealed the homozygous *MEFV*^{P257L} variant.

Patient 2 (III-2) was the younger sister of patient 1. Her symptoms developed at the age of ten, starting with recurrent chest pain (several times per year). Arthralgia/arthritis of the bilateral knees required multiple arthrocentesis in her teens. From the age of 18, she suffered monthly febrile surges with abdominal pain accompanying menstruation and was diagnosed with pyelonephritis or idiopathic peritonitis during each febrile episode. She also occasionally complained of headaches or bilateral conjunctivitis. Given the genetic test result of her brother, she also received the genetic testing at the age

(ROC) curve analysis by assigning clusters 1–5 as disease-associated pathogenic variants and cluster 6 as nonpathogenic/modifier variant (Fig. 3b–d). The optimal thresholds for each cell death were determined as follows,

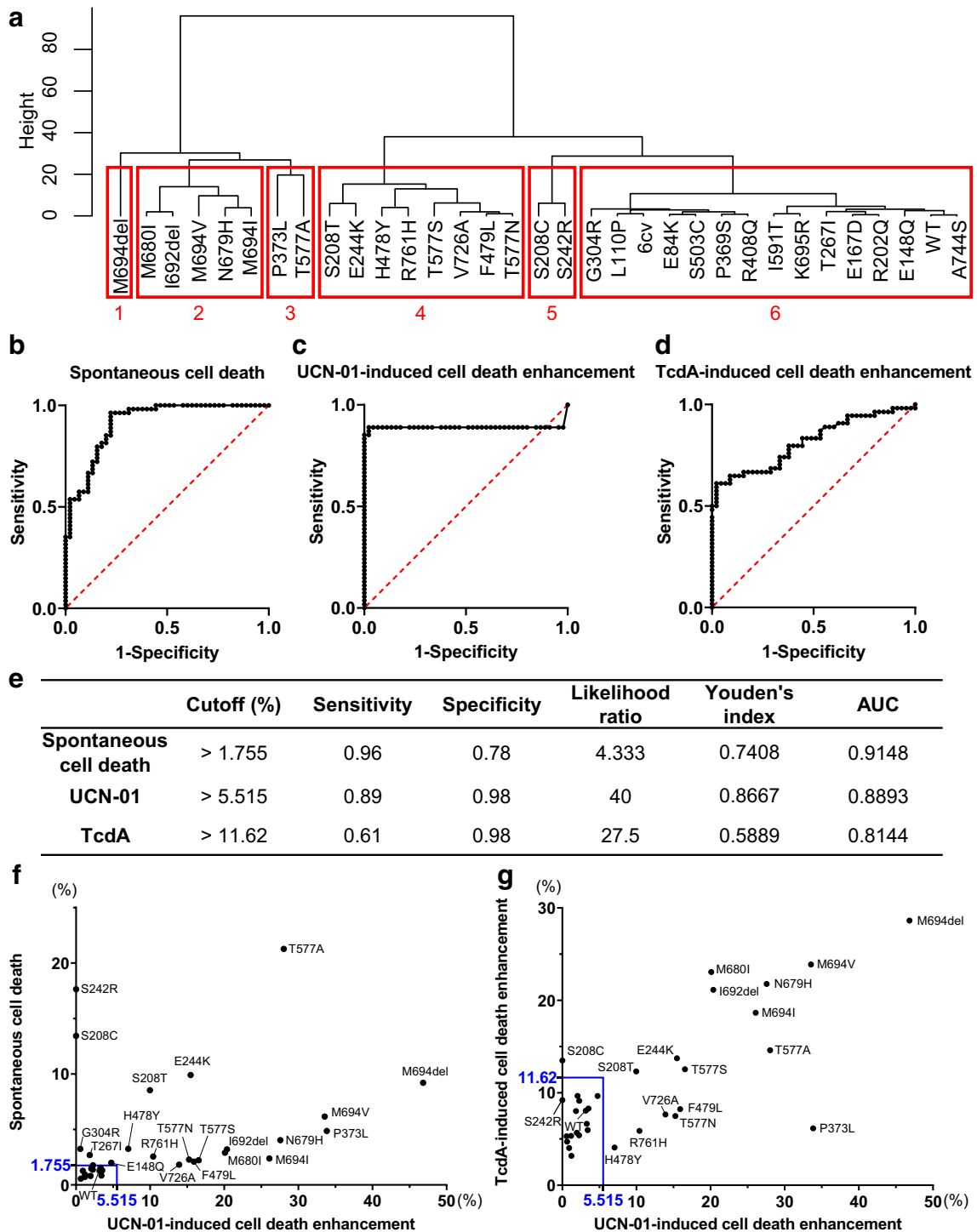


Fig. 3 The mode of cell death induction enables the functional classification of *MEFV* variants. **a** Dendrogram using hierarchical cluster analysis. Variants are classified based on the percentage of spontaneous cell death and enhancement of UCN-01/TcdA-induced cell death. Clusters are divided by red borders. 6cv denotes *MEFV*^{L110P-E148Q-R202Q-P369S-R408Q-S503}. The receiver operating characteristic (ROC) curves for **b** spontaneous cell death, **c** UCN-01-induced cell death enhancement, **d** TcdA-induced cell death enhancement. **e** Cut-off value, sensitivity,

specificity, likelihood ratio, Youden's index, and area under the curve (AUC) for each condition. UCN-01, UCN-01-induced cell death enhancement; TcdA, TcdA-induced cell death enhancement. Scatter plots of mean UCN-01-induced cell death enhancement against **f** mean spontaneous cell death or **g** mean TcdA-induced cell death enhancement. Data represent the mean of three independent experiments. Cut-off values are indicated in blue lines

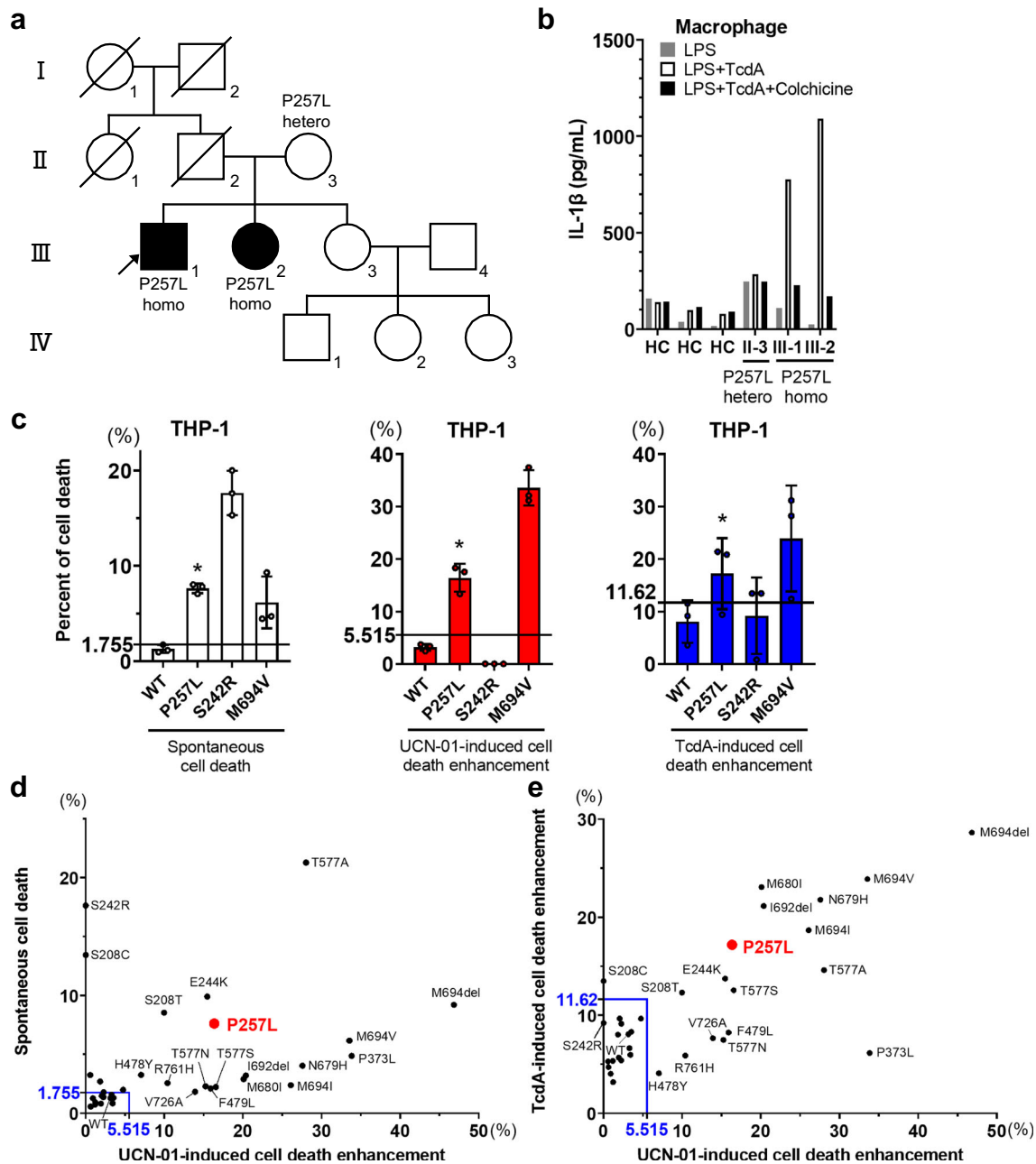


Fig. 4 Homozygous *MEFV*^{P257L} causes autosomal recessive FMF. **a** Pedigree of a family with the *MEFV*^{P257L} variant. **b** IL-1 β secretion from macrophages obtained from homozygous *MEFV*^{P257L} patients, heterozygous mother and healthy controls (HC). LPS-primed macrophages were treated with or without TcdA (1 μ g/mL) and colchicine (100 ng/mL) as indicated. THP-1 based assay to evaluate the pathogenicity of *MEFV*^{P257L}. **c** Percentages of spontaneous and UCN-01/TcdA-induced cell death enhancement by overexpression of *MEFV*^{WT}, *MEFV*^{P257L}, *MEFV*^{S242R}, or *MEFV*^{M694V} variants in THP-1 cells. Cells were stimulated 3 h after

transfection and analyzed 6 h after transfection. The cut-off value for each condition is indicated in black lines, and values above the cut-off are regarded as significantly increased (*). Scatter plots of mean UCN-01-induced cell death enhancement against **d** mean spontaneous cell death or **e** mean TcdA-induced cell death enhancement including *MEFV*^{P257L} variant (red circle). Data represent the mean of three independent experiments. Data represent the average of two or three technical replicates (**b**), the mean \pm standard deviation of three independent experiments (**c**), and the mean of three independent experiments (**d**, **e**)

of 49, which revealed the homozygous *MEFV*^{P257L} variant. Notably, their healthy mother (II-3) carried a heterozygous *MEFV*^{P257L} variant.

To address the pathogenicity of the *MEFV*^{P257L} variant, we first assessed IL-1 β secretion from the patients' macrophages. The TcdA-induced IL-1 β secretion was higher in the patients'

macrophages, when compared to healthy controls and healthy heterozygous mother, which was inhibited by colchicine (Fig. 4b). This pattern was in line with that observed in FMF patients in earlier reports [23, 37]. The THP-1-based functional assay also revealed that the *MEFV*^{P257L} variant induced higher levels of cell death in response to both UCN-01 ($16.353 \pm 2.670\%$) and TcdA ($17.187 \pm 6.749\%$), compared with the calculated cut-off value (Fig. 4c–e), as well as higher IL-1 β secretion compared with the *MEFV*^{WT} (Fig. S8). Taken together, these results suggested that *MEFV*^{P257L} variant could be classified as an autosomal recessive FMF-associated variant, and both patients were finally diagnosed as FMF. Retrospectively, both patients met the Tel Hashomer criteria from their teenage. Subsequent administration of canakinumab, a human anti-IL-1 β monoclonal antibody, combined with colchicine, brought clinical remission in patient 1 (III-1). As to patient 2 (III-2), the administration of colchicine was partially effective and etanercept ameliorated the frequency and severity of the attacks.

In conclusion, our assay, combined with clinical/laboratory data and other functional assays, could help in a more accurate assessment of the pathogenicity of the newly identified or rare *MEFV* variants in the diagnosis of PAADs.

Discussion

In the current era of next-generation sequencing, evaluating the pathogenicity of *MEFV* variants has become important for interpreting genetic test results. However, the majority of reported variants are currently categorized as VOUS, partially due to a lack of reproducible functional assays.

Pyrin is a key component of the pyrin inflammasome, a multiprotein platform that promotes the release of potent inflammatory cytokines (IL-1 β and IL-18) and pyroptotic cell death. RhoA GTPase regulates pyrin activation by phosphorylation at two specific serines, Ser208 and Ser242, via the serine/threonine-protein kinases PKN1/2. GTPase-mediated pyrin phosphorylation results in inhibitory binding by the cellular chaperone protein 14-3-3. However, bacterial toxins, such as TcdA, inactivate RhoA GTPases, leading to pyrin dephosphorylation, 14-3-3 dissociation, and subsequent pyrin inflammasome activation [18–21]. Further, pyrin dephosphorylation by UCN-01, a PKN1/2 inhibitor, has been reported to trigger inflammasome activation in FMF patients [22].

Several patient cell-based assays using TcdA or UCN-01 have been reported based on these mechanisms [22, 23]. However, the co-existence (either in *cis* or in *trans*) of multiple variants in one patient can make it difficult to evaluate the pathogenicity of individual *MEFV* variants using patient-derived cells. In addition, patient cell-dependent assays can be influenced by other factors, such as clinical status (patient in flare or remission), treatment status, or sample condition.

Previously reported in vitro assays utilizing lentiviral-mediated transduction into U-937 monocytic cells [22] or *piggyBac*-mediated iPS cell transfection [37] require multiple experimental steps that make it difficult to evaluate a large number of variants.

In silico predictors, such as rare exome variant ensemble learner (REVEL) [38–40], have been used for evaluating *MEFV* variants. This is a useful tool for improving the classification of many VOUS of *MEFV* gene, especially in combination with clinical and functional reports. However, it still has some discrepancies in clinical or laboratory finding-based classifications, such as the PAAND-associated variants being classified as benign by REVEL scoring. In addition, some rare population-specific variants, such as A744S, were misclassified as pathogenic based on clinical records before the allele frequency database became available [41]. To address these problems, we established a simple THP-1-based functional assay, observing that mutant pyrin overexpression caused caspase-1-dependent pyroptotic cell death upon UCN-01/TcdA stimulation.

In our assay, all the variants in clusters 1 to 4, including FMF-associated exon 10 variants and FMF-like disease-associated variants, showed enhanced cell death in response to UCN-01. These results suggest that FMF-like diseases share a similar pathophysiology to classical FMF, consistent with the notion that PAAD could be recognized as a continuous spectrum, involving a qualitative and quantitative molecular gradient ranging from classical FMF to autosomal dominant FMF-like diseases.

Notably, the TcdA response of V726A and R761H, which are exon 10 FMF-associated variants classified in cluster 4, was comparable to that of WT, which clearly differed from those of classical exon 10 FMF-associated variants in clusters 1 and 2. These two variants are generally associated with a milder phenotype and are known to be observed as wild type sequence in some non-human primates and non-primates [42, 43]. Thus, these two variants, which evolutionarily reappeared in human, might have different characters from other classical exon 10 variants. In addition, non-exon 10 FMF-like disease-associated variants in cluster 4, such as H478Y and T577S/N, showed normal TcdA-response, which was different from exon 10 FMF-associated variants. This provides insights into the genetic and clinical differences between classical FMF and FMF-like diseases, such as the mode of inheritance (autosomal recessive or autosomal dominant) and symptoms (duration or degree of fever). These differences might arise from the evolutionary conservation of different pyrin domains. FMF-associated exon 10 variants are located in B30.2 domain, which recently appeared during primate evolution, while FMF-like disease-associated variants are located in the other evolutionarily conserved domains. However, further studies are required to determine whether these are true biological differences or only observational phenomena unique to our analysis.

Previously, we questioned the pathogenicity of *MEFV*^{T577N} variant based on the negative result from iPS-derived macrophages. Upon TcdA stimulation, iPS-derived macrophages transfected with *MEFV*^{T577N} secreted comparable amounts of IL-1 β to those transfected with *MEFV*^{WT} [37]. In silico analysis predicted *MEFV*^{T577N} as benign [40]. However, the clinical phenotypes [35] strongly suggested pathogenic association with FMF-like disease. In this study, *MEFV*^{T577N} significantly increased UCN-01-induced cell death compared to *MEFV*^{WT} (Fig. 2b), while it exhibited similar degrees of spontaneous and TcdA-induced cell death compared to *MEFV*^{WT} (Fig. 2a, c). These results suggest that *MEFV*^{T577N} could be categorized as an FMF-like disease-associated pathogenic variant based on the hyper-responsiveness to UCN-01.

Taken together, UCN-01-induced cell death enhancement might reflect the nature of FMF- and FMF-like disease-associated *MEFV* variants better than that induced by TcdA in this assay. This seems reasonable because UCN-01 directly targets the pyrin dephosphorylation which mainly controls the pyrin inflammasome activation in FMF patients [22], while TcdA represents one of the many agonists which indirectly induce pyrin dephosphorylation. Also, the degree of UCN-01-induced cell death enhancement might correlate with the clinical severity of the variant. M694V, which is often associated with severe phenotype, showed higher degrees of UCN-01-induced cell death compared to the variants with milder phenotypes such as V726A [34] and M680I [44]. Among the three variants affecting the T577 residue, T577A showed stronger UCN-01-induced cell death enhancement than T577N/S, which might correlate with the treatment resistance reported in T577A cases [12].

All 14-3-3 binding site-associated variants induced high levels of cell death in the absence of pyrin agonist stimulation, possibly reflecting the spontaneous pyrin inflammasome activation, as reported previously [9, 10]. Interestingly, S208T and E244K in cluster 3, but not S208C and S242R in cluster 5, showed hyper-response to UCN-01, suggesting the existence of a functional difference among the variants affecting the same domain. Only S242R and E244K are reported as PAAND-associated variants in clinical settings, while S208T/C variants are linked to other autoinflammatory conditions. Further analyses and clinical experience are required to clarify whether these differences are significant.

We detected no substantial increase in spontaneous cell death and TcdA/UCN-01-induced cell death enhancement among the variants in cluster 6 (WT and E84K, L110P, E148Q, E167D, R202Q, T267I, G304R, P369S, R408Q, S503C, I591T, K695R, or A744S). However, E148Q, R202Q, T267I, and G304R showed slightly increased spontaneous cell death, above the cut-off value. In addition, H478Y, a non-exon 10 FMF-like disease-associated variant, induced slightly higher levels of UCN-01 response above the cut-off value. There has been only a single case report

describing heterozygous *MEFV*^{H478Y} patients [11]. This assay may not be suitable for detecting subtle effects or unknown pathogenic mechanisms that underlie the clinical condition of these patients. Further clinical and experimental data are required to conclude the causal relationship of these borderline variants.

This study has a few limitations. First, although endogenous WT pyrin expression was almost negligible in THP-1 cells compared to the transfected variants, we cannot completely exclude the possibility that residual pyrin affected our results. In contrast, transgene expression may not correspond to the physiological pyrin expression and might overrepresent the result. Second, we did not evaluate the effect of variants in the *trans* state, as is often experienced in the real-world FMF patients. Future co-expression experiments could provide important insights into the effect of gene dose or the *trans*-acting effect of *MEFV* variants. Third, our clustering is based on the results from an arbitrarily selected cell line, 32 *MEFV* variants, and 2 agonists, which might not represent the diverse cell types involved in PAAD pathogenesis, the diverse spectrum of *MEFV* variants, and the natural triggers of pyrin inflammasome, respectively. Therefore, a comprehensive analysis of other cell types, variants, or agonists is required for an accurate understanding of pyrin inflammasome activation. Lastly, the THP-1-based assay evaluates variants independently of the patient status, co-existence of the other variants, or genetic background. This could be a disadvantage in the evaluation of a PAAD that manifests because of complex interplay among the genetic or environmental factors. Therefore, diagnosis of PAAD should not be established based on a single assay, and therefore, our functional assay needs to be framed with a balanced genotype-phenotype correlation.

In conclusion, we analyzed 32 *MEFV* variants and evaluated those pathogenicity based on the degrees of spontaneous and TcdA/UCN-01-induced cell death. These variants were categorized into 6 distinct clusters, which might partly explain the diverse clinical entity of PAADs. The strength of cell death induction by each variant seemed to correlate with its clinical severity. This assay might be helpful in the diagnosis of the PAAD patients with VOUS or previously unreported variants, as in the case of *MEFV*^{P257L} variant. Therefore, this assay can help in functional evaluation of *MEFV* variants in a simple manner and can be used for the accurate diagnosis and better understanding of PAADs when integrated with precise clinical descriptions as well as other laboratory/experimental data.

Supplementary Information The online version contains supplementary material available at <https://doi.org/10.1007/s10875-021-01021-7>.

Acknowledgements We would like to thank *Editage* (www.editage.com) for English language editing and Kumi Kodama for technical assistance.

Author Contribution YH, YM, KI, and TY designed and wrote the manuscript. YH, YM, TS, and TT performed the experiments and analyzed the data. HN, KN, and HM collected clinical data and provided samples of patients and relatives for analyses. HN, KN, HM, MI, TM, HN, HS, EH, OO, JT, and RN provided crucial conceptual inputs and helped in writing the manuscript. OO performed the next-generation sequencing and data analyses. All authors reviewed, contributed, and approved the final manuscript.

Funding This research was supported by the following grants: Grants-in-Aids for Young Scientists (grant JP19K17293 to KI, JP20K16889 to TS, and JP20K16924 to YH), Grants-in-Aids for Scientific Research (C) (grant JP19K08320 to T.T.), Health Labor Sciences Research Grants for Research on Intractable Diseases from the Ministry of Health, Labor and Welfare (MHLW) of Japan (H29-Nanchi-Ippan-020 and JPMH20317089 to KI, TY, and RN); the Practical Research Project for Rare/Intractable Diseases from the Japan Agency for Medical Research and Development (AMED) (JP19ek0109200 and JP20ek0109477 to KI).

Availability of Data and Material The datasets generated during and/or analyzed during the current study are available from the corresponding author on reasonable request.

Code Availability Not applicable.

Declarations

Ethics Approval This study is conducted in compliance with the Declaration of Helsinki. In addition, all experiments involving human subjects were conducted in accordance with local regulations and were approved by the ethics committee of Kyoto University Hospital (protocols G1091, G0729, G0457, G0432).

Consent to Participate Informed consent was obtained from all participants including in this study.

Consent for Publication Patients signed informed consent regarding publishing their data.

Conflicts of Interest The authors declare no competing interests.

References

- Heller H, Sohar E, Sherf L. Familial Mediterranean fever. *M Archives Intern Medicine*. 1958;102:50–71.
- Schnappauf O, Chae JJ, Kastner DL, Aksentjevich I. The Pyrin Inflammasome in health and disease. *Front Immunol*. 2019;10:1745.
- Livneh A, Langevitz P, Zemer D, Zaks N, Kees S, Lidar T, et al. Criteria for the diagnosis of familial mediterranean fever. *Arthritis Rheum*. 1997;40:1879–85.
- Shinar Y, Obici L, Aksentjevich I, Bennetts B, Austrup F, Ceccherini I, et al. Guidelines for the genetic diagnosis of hereditary recurrent fevers. *Ann Rheum Dis*. 2012;71:1599–605.
- Ozen S, Bilginer Y. A clinical guide to autoinflammatory diseases: familial Mediterranean fever and next-of-kin. *Nat Rev Rheumatol*. 2014;10:135–47.
- Consortium TIF. Ancient missense mutations in a new member of the RoRet gene family are likely to cause familial Mediterranean fever. *Cell*. 1997;90:797–807.
- Consortium TFF, Bernot A, Clepet C, Dasilva C, Devaud C, Petit J-L, et al. A candidate gene for familial Mediterranean fever. *Nat Genet*. 1997;17:25–31.
- Touitou I. The spectrum of familial Mediterranean fever (FMF) mutations. *Eur J Hum Genet*. 2001;9:473–83.
- Masters SL, Lagou V, Jéru I, Baker PJ, Eyck LV, Parry DA, et al. Familial autoinflammation with neutrophilic dermatosis reveals a regulatory mechanism of pyrin activation. *Sci Transl Med*. 2016;8:332ra45–5.
- Moghaddas F, Llamas R, Nardo DD, Martinez-Banaclocha H, Martinez-Garcia JJ, Mesa-del-Castillo P, et al. A novel pyrin-associated autoinflammation with neutrophilic dermatosis mutation further defines 14-3-3 binding of pyrin and distinction to familial Mediterranean fever. *Ann Rheum Dis*. 2017;76:2085–94.
- Aldea A, Campistol JM, Arostegui JI, Rius J, Maso M, Vives J, et al. A severe autosomal-dominant periodic inflammatory disorder with renal AA amyloidosis and colchicine resistance associated to the MEFV H478Y variant in a Spanish kindred: an unusual familial Mediterranean fever phenotype or another MEFV-associated periodic inflammatory disorder? *Am J Med Genet A*. 2004;124A:67–73.
- Stoffels M, Szperl A, Simon A, Netea MG, Plantinga TS, van Deuren M, et al. MEFV mutations affecting pyrin amino acid 577 cause autosomal dominant autoinflammatory disease. *Ann Rheum Dis*. 2014;73:455–61.
- Rowczenio DM, Youngstein T, Trojer H, Omoyinmi E, Baginska A, Brogan P, et al. British kindred with dominant FMF associated with high incidence of AA amyloidosis caused by novel MEFV variant, and a review of the literature. *Rheumatology*. 2019;59:554–8.
- Ben-Chetrit E, Gattorno M, Gul A, Kastner DL, Lachmann HJ, Touitou I, et al. Consensus proposal for taxonomy and definition of the autoinflammatory diseases (AIDs): a Delphi study. *Ann Rheum Dis*. 2018;77:1558–65.
- Shinar Y, Ceccherini I, Rowczenio D, Aksentjevich I, Arostegui J, Ben-Chetrit E, et al. ISSAID/EMQN best practice guidelines for the genetic diagnosis of monogenic autoinflammatory diseases in the next-generation sequencing era. *Clin Chem*. 2020;66:525–36.
- Boursier G, Hentgen V, Sarabay G, Koné-Paut I, Touitou I. The changing concepts regarding the Mediterranean fever gene: toward a spectrum of pyrin-associated autoinflammatory diseases with variable heredity. *J Pediatr*. 2019;209:12–16.e1.
- Milhavet F, Cuisset L, Hoffman HM, Slim R, El-Shanti H, Aksentjevich I, et al. The infevers autoinflammatory mutation online registry: update with new genes and functions. *Hum Mutat*. 2008;29:803–8.
- Xu H, Yang J, Gao W, Li L, Li P, Zhang L, et al. Innate immune sensing of bacterial modifications of rho GTPases by the pyrin inflammasome. *Nature*. 2014;513:237–41.
- Park YH, Wood G, Kastner DL, Chae JJ. Pyrin inflammasome activation and RhoA signaling in the autoinflammatory diseases FMF and HIDS. *Nat Immunol*. 2016;17:914–21.
- Gao W, Yang J, Liu W, Wang Y, Shao F. Site-specific phosphorylation and microtubule dynamics control pyrin inflammasome activation. *Proc National Acad Sci*. 2016;113:E4857–66.
- Gorp HV, Saavedra PHV, de Vasconcelos NM, Opendbosch NV, Walle LV, Matusiak M, et al. Familial Mediterranean fever mutations lift the obligatory requirement for microtubules in pyrin inflammasome activation. *Proc National Acad Sci*. 2016;113:14384–9.
- Magnotti F, Lefeuve L, Benezech S, Malsot T, Waeckel L, Martin A, et al. Pyrin dephosphorylation is sufficient to trigger inflammasome activation in familial Mediterranean fever patients. *Embo Mol Med*. 2019;11:e10547.

23. Gorp HV, Huang L, Saavedra P, Vuylsteke M, Asaoka T, Prencipe G, et al. Blood-based test for diagnosis and functional subtyping of familial Mediterranean fever. *Ann Rheum Dis.* 2020;79:960–8.
24. Magnotti F, Malsot T, Georgin-lavialle S, Abbas F, Martin A, Belot A, et al. Fast diagnostic test for familial Mediterranean fever based on a kinase inhibitor. *Ann Rheum Dis.* 2020;annrheumdis-2020-218366.
25. Charrad M, Ghazzali N, Boiteau V, Niknafs A. NbClust: an R package for determining the relevant number of clusters in a data set. *J Stat Softw.* 2014;61:1–36.
26. Fujisawa A, Kambe N, Saito M, Nishikomori R, Tanizaki H, Kanazawa N, et al. Disease-associated mutations in CIAS1 induce cathepsin B-dependent rapid cell death of human THP-1 monocyte cells. *Blood.* 2007;109:2903–11.
27. Tanaka N, Izawa K, Saito MK, Sakuma M, Oshima K, Ohara O, et al. High incidence of NLRP3 somatic mosaicism in patients with chronic infantile neurologic, cutaneous, articular syndrome: results of an international multicenter collaborative study. *Arthritis Rheum.* 2011;63:3625–32.
28. Nakagawa K, Gonzalez-Roca E, Souto A, Kawai T, Umabayashi H, Campistol JM, et al. Somatic NLRP3 mosaicism in Muckle-Wells syndrome. A genetic mechanism shared by different phenotypes of cryopyrin-associated periodic syndromes. *Ann Rheum Dis.* 2013;74:603–10.
29. Ozkaya S, Butun SE, Findik S, Atici A, Dirican A. A very rare cause of Pleuritic chest pain: bilateral Pleuritis as a first sign of familial Mediterranean fever. *Case Reports Pulmonol.* 2013;2013:315751.
30. Kishida D, Nakamura A, Yazaki M, Tsuchiya-Suzuki A, Matsuda M, Ikeda S. Genotype-phenotype correlation in Japanese patients with familial Mediterranean fever: differences in genotype and clinical features between Japanese and Mediterranean populations. *Arthritis Res Ther.* 2014;16:439.
31. Migita K, Agematsu K, Yazaki M, Nonaka F, Nakamura A, Toma T, et al. Familial Mediterranean fever. *Medicine.* 2014;93:158–64.
32. Migita K, Izumi Y, Jiuchi Y, Iwanaga N, Kawahara C, Agematsu K, et al. Familial Mediterranean fever is no longer a rare disease in Japan. *Arthritis Res Ther.* 2016;18:175.
33. Rowczenio DM, Iancu DS, Trojer H, Gilbertson JA, Gillmore JD, Wechalekar AD, et al. Autosomal dominant familial Mediterranean fever in Northern European Caucasians associated with deletion of p.M694 residue—a case series and genetic exploration. *Rheumatology.* 2016;56:209–13.
34. Cekin N, Akyurek ME, Pinarbasi E, Ozen F. MEFV mutations and their relation to major clinical symptoms of familial Mediterranean fever. *Gene.* 2017;626:9–13.
35. Nakaseko H, Iwata N, Izawa K, Shibata H, Yasuoka R, Kohagura T, et al. Expanding clinical spectrum of autosomal dominant pyrin-associated autoinflammatory disorder caused by the heterozygous MEFV p.Thr577Asn variant. *Rheumatology.* 2018;58:182–4.
36. Hong Y, Standing ASI, Nanthapisal S, Sebire N, Jolles S, Omoyinmi E, et al. Autoinflammation due to homozygous S208 MEFV mutation. *Ann Rheum Dis.* 2019;78:571–3.
37. Shiba T, Tanaka T, Ida H, Watanabe M, Nakaseko H, Osawa M, et al. Functional evaluation of the pathological significance of MEFV variants using induced pluripotent stem cell-derived macrophages. *J Allergy Clin Immunol.* 2019;144:1438–1441.e12.
38. Stella A, Portincasa P. Comment on: improvement of MEFV gene variants classification to aid treatment decision making in familial Mediterranean fever: reply. *Rheumatology.* 2019;59:911–2.
39. Jamilloux Y, Magnotti F. Comment on: improvement of MEFV gene variants classification to aid treatment decision making in familial Mediterranean fever. *Rheumatology.* 2019;59:910–1.
40. Accetturo M, D'Uggento AM, Portincasa P, Stella A. Improvement of MEFV gene variants classification to aid treatment decision making in familial Mediterranean fever. *Rheumatology.* 2019;59:754–61.
41. Alsubaie L, Alkhalaf R, Aloraini T, Amoudi M, Swaid A, Mutairi FA, et al. MEFV c.2230G>T p.(Ala744Ser) rs61732874 previously misclassified as pathogenic variant due to lack of a population specific database. *Ann Hum Genet.* 2020;84:370–9.
42. Schaner P, Richards N, Wadhwa A, Aksentijevich I, Kastner D, Tucker P, et al. Episodic evolution of pyrin in primates: human mutations recapitulate ancestral amino acid states. *Nat Genet.* 2001;27:318–21.
43. Stella A, Lamkanfi M, Portincasa P. Familial Mediterranean fever and COVID-19: friends or foes? *Front Immunol.* 2020;11:574593.
44. Gangemi S, Manti S, Procopio V, Casciaro M, Salvo ED, Cutrupi M, et al. Lack of clear and univocal genotype-phenotype correlation in familial Mediterranean fever patients: a systematic review. *Clin Genet.* 2018;94:81–94.

Publisher's Note Springer Nature remains neutral with regard to jurisdictional claims in published maps and institutional affiliations.

Reproduced with permission from Springer Nature

Supplemental data

Journal of Clinical Immunology

Rapid flow cytometry-based assay for the functional classification of *MEFV* variants

Yoshitaka Honda, MD^{1*}, Yukako Maeda, MD^{1*}, Kazushi Izawa, MD, PhD^{1**}, Takeshi Shiba, MD, PhD^{1,2}, Takayuki Tanaka, MD, PhD^{1,3}, Haruna Nakaseko, MD⁴, Keisuke Nishimura, MD, PhD⁵, Hiroki Mukoyama, MD⁶, Masahiko Isa-Nishitani, MD¹, Takayuki Miyamoto, MD¹, Hiroshi Nihira, MD¹, Hirofumi Shibata, MD, PhD¹, Eitaro Hiejima, MD, PhD¹, Osamu Ohara, PhD⁷, Junko Takita, MD, PhD¹, Takahiro Yasumi, MD, PhD^{1**}, Ryuta Nishikomori, MD, PhD⁸

¹ Department of Pediatrics, Kyoto University Graduate School of Medicine, Kyoto, Japan

² Department of Pediatrics, Tenri Hospital, Tenri, Japan

³ Department of Pediatrics, Otsu Red Cross Hospital, Otsu, Japan

⁴ Department of Infection and Immunology, Aichi Children's Health and Medical Center, Obu, Japan

⁵ Department of Endocrinology and Rheumatology, Kurashiki Central Hospital, Kurashiki, Japan

⁶ Department of Rheumatology and Clinical Immunology, Kyoto University Graduate School of Medicine, Kyoto, Japan

⁷ Kazusa DNA Research Institute, Kisarazu, Japan

⁸ Department of Pediatrics and Child Health, Kurume University School of Medicine, Kurume, Japan

*These authors contributed equally to this work

**Corresponding authors:

Kazushi Izawa, MD, PhD

Department of Pediatrics, Faculty of Medicine, Kyoto University, 54 Kawahara-cho, Shogoin, Sakyo-ku, Kyoto 606-8507, Japan

E-mail: kizawa@kuhp.kyoto-u.ac.jp

Phone: +81-75-751-3290, FAX: +81-75-751-4208

Takahiro Yasumi, MD, PhD

Department of Pediatrics, Faculty of Medicine, Kyoto University, 54 Kawahara-cho, Shogoin, Sakyo-ku, Kyoto 606-8507, Japan

E-mail: yasumi@kuhp.kyoto-u.ac.jp

Phone: +81-75-751-3290, FAX: +81-75-751-4208

Supplementary methods

Immunofluorescence

THP-1 cells (1×10^6) were transfected with 500 ng of eGFP-*MEFV* plasmids by nucleofector device Iib and kit V (Lonza, Basel, Switzerland). Cells were stimulated with TcdA (Sigma-Aldrich, St. Louis, MO, US) or UCN-01 (Sigma-Aldrich) 3 hours after transfection. Three hours after stimulation, cells were attached to MAS-04 coated slides (Matsunami, Osaka, Japan) using a Cytospin 4 Cyto centrifuge (Thermo Fisher Scientific, Waltham, MA, US), fixed with 4 % paraformaldehyde (FUJIFILM Wako, Osaka, Japan), and permeabilized with 0.1% Triton X-100 (Nacalai, Kyoto, Japan). Cells were incubated with an anti-ASC antibody (# AG-25B-0006-C100; 1:400; Adipogen, Liestal, Switzerland) and then with an Alexa Fluor 594-labeled antibody to rabbit IgG (# A-11012; 1:1000; Thermo Fisher Scientific). Nuclei were stained with 4',6-diamidino-2-phenylindole (Dojindo, Kumamoto, Japan). Cells were examined using a BZ-X710 fluorescence microscope (Keyence, Osaka, Japan), and the percentage of ASC speck-positive cells among GFP-positive cells was calculated.

IL-1 β secretion from THP-1 cells

THP-1 cells (1×10^6) were transfected with 500 ng of eGFP-*MEFV* plasmids by nucleofector device Iib and kit V (Lonza). Immediately after nucleofection, cells were seeded into 96 well plate (6.5×10^4 cells per well) and were primed with LPS (100 ng/mL) (Sigma-Aldrich) and PMA (10 ng/mL) (FUJIFILM Wako). After 3 hours of LPS priming, cells were treated with TcdA (1 μ g/mL) or UCN-01 (10 μ M) or left untreated. After 3 hours of stimulation, supernatants were collected. The IL-1 β concentration was measured in technical duplicates or triplicates by using the Bio-Plex Pro Human Cytokine Assay (Bio-Rad Laboratories, Hercules, CA, US).

Genetic analysis

Two patients (III-1 and III-2 in Fig. 4a) and their healthy mother (II-3) had received next-generation sequencing based panel gene tests for *MEFV*, *CECRI*, *COPA*, *FAM105B*, *HMOX1*, *IL1RN*, *MVK*, *NLRC4*, *NLRP12*, *NLRP3*, *NOD2*, *PLCG2*, *POMP*, *PSMA3*, *PSMB4*, *PSMB8*, *PSMB9*, *PSTPIP1*, *RBCK1*, *RNF31*, *TNFAIP3*, and *TNFRSF1A*. We detected homozygous *MEFV*^{P257L} variant in III-1 and III-2, heterozygous *MEFV*^{P257L} in II-3, respectively. No pathogenic or rare variant was detected in other autoinflammatory disease associated genes listed above.

For healthy controls, all the coding regions of *MEFV* gene were examined by Sanger sequencing, and there was no *MEFV* variant. Detailed information for the primers and PCR is available upon request.

Generation of caspase-1 knockout THP-1 cells

The *CASP1* gene was knocked out using the Clustered Regularly Interspaced Short Palindromic Repeats (CRISPR)/Cas9 system. Single guide RNA constructs targeting exon 6 of the *CASP1* gene were introduced into the lentiCRISPR v2 vector (Addgene, Watertown, MA, US) and viral particles were generated using a Lenti-Pac HIV Expression Packaging Kit (Genecopoeia, Rockville, MD, US) according to the manufacturer's instructions. The viral supernatant was added to 3×10^6 THP-1 cells and supplemented with 8 μ g/mL of polybrene before being centrifuged for 45 min at $800 \times g$ at 32 °C, incubated at 37 °C for 4 h, and washed and reseeded in fresh RPMI. After 72 h, 1 μ g/mL of puromycin was added and surviving cells were diluted and dispersed into 96-well plates for a single-clone selection.

Western blotting

THP-1 cells (1×10^6) were lysed in Mammalian Protein Extraction Reagent (M-PER; Thermo Fisher Scientific) supplemented with a Protease Inhibitor Cocktail (Nacalai Tesque, Kyoto, Japan). Total protein (10 μ g) was separated by SDS-PAGE and transferred to a polyvinylidene difluoride membrane. Membranes were blocked with Tris-buffered saline supplemented with 0.1 % Tween 20 and 5 % nonfat dried milk and incubated at room temperature with primary antibodies for 1 h, and then incubated at room temperature with the appropriate horseradish peroxidase-conjugated secondary antibodies for 1 h (Jackson ImmunoResearch, West Grove, PA, US). Membranes were then incubated with Clarity Western ECL Substrate (Bio-Rad, Hercules, CA, US) and signals were acquired using ChemiDoc Imaging System (Bio-Rad). The following antibodies

were used: mouse anti-GFP (# sc-9996; 1:200; Santa Cruz, Dallas, TX, US), rabbit anti-pyruvate kinase M2 (# AG-25B-0020-C100; 1:1000; Adipogen, Liestal, Switzerland), rabbit anti-caspase-1 (# 3866; 1:1000; Cell Signaling Technology, Danvers, MA, US), and mouse anti- β -actin (# 010-27841; 1:2000; FUJIFILM Wako).

Table S1 List of primer sequences

	HGVS protein name	HGVS sequence name	forward primer sequence	reverse primer sequence
E84K	p.(Glu84Lys)	c.250G>A	CAACCAGCGCTGCTGGCCAAGGAGCTCCACAGGGCAG	CTGCCCTGTGGAGCTCCTTGGCCAGCAGGGCGTGGTTG
L110P	p.(Leu110Pro)	c.329T>C	CCGCAGCGTCCAGCTCCCCGGGGGAGAACAAGCCC	GGGCTTGTCTCCCCGGGGAGCTGGACGCTGCGG
E148Q	p.(Glu148Gln)	c.442G>C	CCTCCCGCCTGGGGCTGGCTGC	GCAGCCAGCCCCAGGCCGGGAGG
E167D	p.(Glu167Asp)	c.501G>C	CTTGCCCTGCGCGTCCAGGCCGTCGAGGCCCTTCTCTC	GAGAGAAGGCCCTCGGACGGCCTGGACGCGCAGGGCAAG
R202Q	p.(Arg202Gln)	c.605G>A	GGCCAGGCCGAGGTCCAGCTGCGCAGAAACGCCAGC	GCTGGCGTTTCTGCGCAGCTGGACCTCGGCCTGGCC
S208C	p.(Ser208Cys)	c.622A>T	GGCTGCGCAGAAACGCCCTGCTCCGCGGGGAGGCTGC	GCAGCCTCCCCGCGGAGCAGGCGTTTCTGCGCAGCC
S208T	p.(Ser208Thr)	c.623G>C	CTGCGCAGAAACGCCACCTCCGCGGGGAGGCTG	CAGCCTCCCCGCGGAGGTGGCGTTTCTGCGCAG
S242R	p.(Ser242Arg)	c.726C>G	GAAAGATGCGACCTAGAAGGCTTGAGGTCCACATTTCTAC	GTAGAAATGGTGACCTCAAGCCTTCTAGGTTCGCATCTTC
E244K	p.(Glu244Lys)	c.730G>A	GATGCGACCTAGAAGCCTTAAGGTCCACATTTCTACAGGG	CCCTGTAGAAATGGTGACCTTAAGGCTTCTAGGTTCGCATC
P257L	p.(Pro257Leu)	c.770C>T	AGTCAGGAGAATTTCTAGATTTGCGGGCGCCTTC	GAAGGCGCCCCGAAATCTAGAAATTCTCTGACT
T267I	p.(Thr267Ile)	c.800C>T	GACTCTAGAGGAAAAGATAGCTGCGAATCTGGACTCG	CGAGTCCAGATTCGCTATCTTTTCTCTAGAGTC
G304R	p.(Gly304Arg)	c.910G>A	CCAGAACATTCCGTCACCAGAAGGCCACCAGACACGGC	GCCGTGTCTGGTGGCCTTCTGGTGACCGAATGTTCTGG
P369S	p.(Pro369Ser)	c.1105C>T	GAGCCCGGAAGCCTAAGCTCCCAGCCCTGCCACAG	CTGTGGCAGGGGCTGGGAGCTTAGGCTTCCCGGGCTC
P373L	p.(Pro373Leu)	c.1118C>T	GCCCCAGCCCCTGCTACAGTGTAAGGCCACC	GGTGGCGCTTACTACTGTAGCAGGGGCTGGGGC
R408Q	p.(Arg408Gln)	c.1223G>A	GGAGCACCAAGGCCACCAGGTGCGCCATTGAGGAGG	CCTCCTCAATGGGGCGCACCTGGTGGCCTTGGTGTCTC
H478Y	p.(His478Tyr)	c.1432C>T	CCTGGAGCAGCAAGAGTATTTCTTTGTGGCCTCAC	CCTGGAGCAGCAAGAGTATTTCTTTGTGGCCTCAC
F479L	p.(Phe479Leu)	c.1437C>G	GGAGCAGCAAGAGCATTGTTTGTGGCCTCACTGGAGG	CCTCCAGTGAGGCCACAAACAAATGCTCTTGCTGTCTC
S503C	p.(Ser503Cys)	c.1508C>G	CATATGACACCCGCGTATGCCAGGACATCGCCCTGC	GCAGGGCGATGCTCTGGCATAACGCGGTGTATATG
T577A	p.(Thr577Ala)	c.1729A>G	GCACAAAGTACTTCTCAGAAGCCCTGCGTTCAGAAATGG	CCATTTCTGAACGCAGGCTTCTGAGAAGTACTTTGTGC
T577N	p.(Thr577Asn)	c.1730C>A	TCTGAACGCAGGTTTTCTGAGAAGTACTTTGTGCTC	GAGCACAAAGTACTTCTCAGAAAACCTGCGTTCAGA
T577S	p.(Thr577Ser)	c.1729A>T	GCACAAAGTACTTCTCAGAATCCCTGCGTTCAGAAATGG	CCATTTCTGAACGCAGGATTCTGAGAAGTACTTTGTGC
I591T	p.(Ile591Thr)	c.1772T>C	CAATGTTCCAGAGCTGACTGGCGCTCAGGCACATG	CATGTGCTGAGCGCCAGTCAGCTCTGGAACATTG
N679H	p.(Asn679His)	c.2035A>C	GGCGACAGAGTCATGTGCCCTTTCTGCTTATG	CATAAGCAGGAAAGGGCACATGACTCTGTCCGC
M680I	p.(Met680Ile)	c.2040G>A	GCAGGAAAGGGAACATAACTCTGTGCGCCAGAGAATGG	CCATTTCTGGCGACAGAGTTATGTTCCCTTTCTCTGC
I692del	p.(Ile692del)	c.2076_2078del	1) CAGATATCCAGCACAGTGGCGGCCGATGGCTAAGACCCCTAGTG 2) GGGTGGTGTGATGATGAAGGAAAATGAGTACC	1) TTCCTCATCATCACCACCCAGTAAGCCATTC 2) TTAAACGGGCCCTCTAGACTCGAGTTACTTGTACAGCTCGTC
M694I	p.(Met694Ile)	c.2082G>A	GGTACTGGGTGGTGATAATGATAAAGGAAAATGAGTACC	GGTACTCATTTTCTTTATCATTATCACCACCCAGTAGCC
M694V	p.(Met694Val)	c.2080A>G	GGTACTCATTTTCTTACCATTATCACCACCCAGTAG	CTACTGGGTGGTGATAATGGTGAAGGAAAATGAGTACC
M694del	p.(Met694del)	c.2081_2083del	CTACTGGGTGGTGATAATGAAGGAAAATGAGTACCAG	CTGGTACTCATTTTCTTATTATCACCACCCAGTAG
K695R	p.(Lys695Arg)	c.2084A>G	GGGTGGTGATAATGATGAGGGAAAATGAGTACCAGGCG	CGCCTGGTACTCATTTTCCCTCATATTATCACCACCC
V726A	p.(Val726Ala)	c.2177T>C	CTTCGTGGACTACAGAGCTGGAAGCATCTCCTTTTAC	GTAAAAGGAGATGCTTCCAGCTCTGTAGTCCACGAAG
A744S	p.(Ala744Ser)	c.2230G>T	GATCCACATCTATACATTCTCCAGCTGCTTTTCTCTG	CAGAGAAAGAGCAGCTGGAGATGTATAGATGTGGGATC
R761H	p.(Arg761His)	c.2282G>A	CTTCAGCCCTGGGACACATGATGGAGGGAAGAACAC	GTGTCTTCCCTCCATCATGTGTCCAGGGCTGAAG

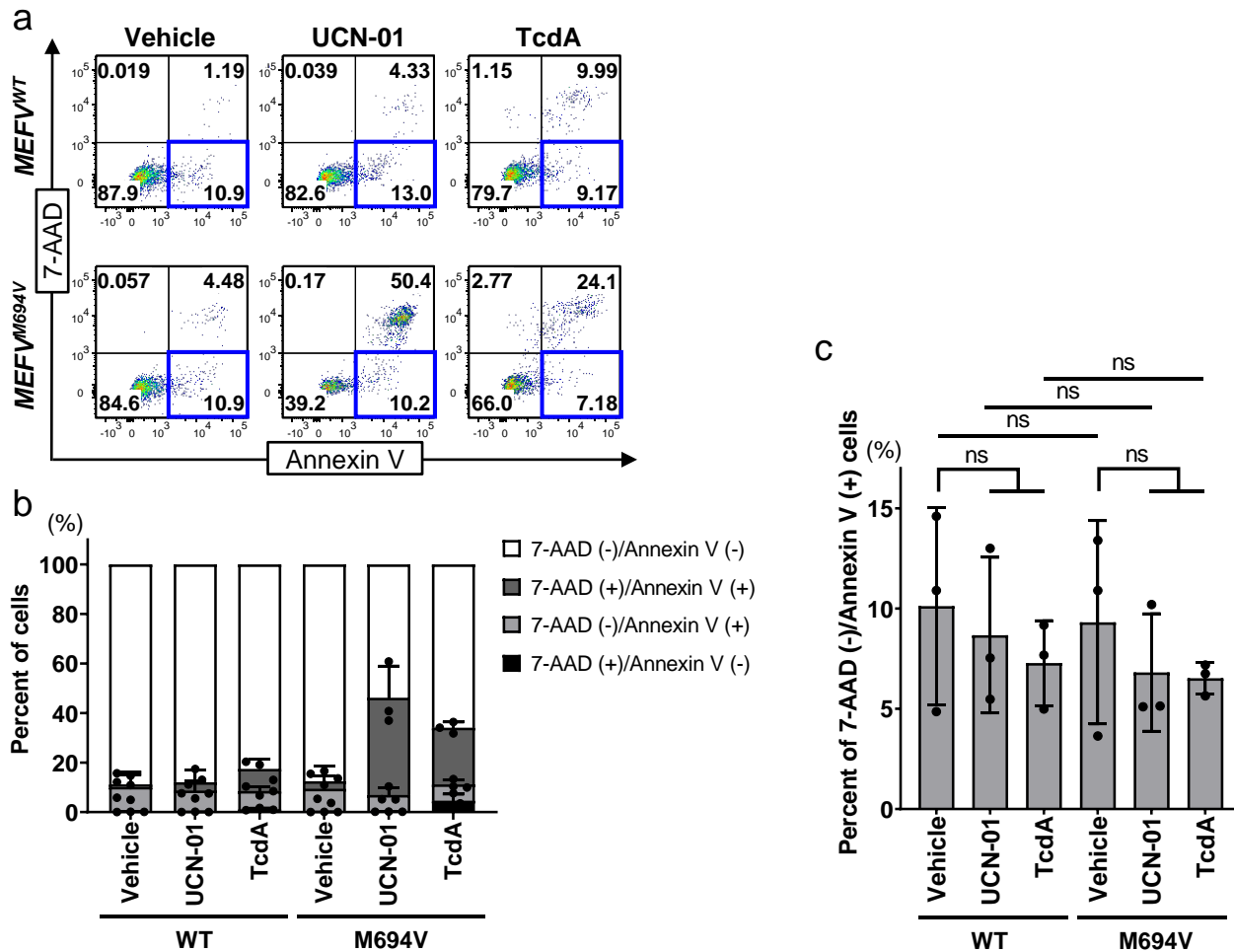
Table S2 List of analyzed variants

	Exon	domain	HGVS protein name	HGVS sequence name	rs number	Allele frequency in gnomAD v2.1.1			Pathogenicity score /Status in Infevers (17)	Classification in the new guidelines (15)
						Total	East Asian	European (non-Finnish)		
E84K	1	PYD	p.(Glu84Lys)	c.250G>A	rs150819742	0.0001085	0.001197	0.000	Likely pathogenic/PROVISIONAL	
L110P	2		p.(Leu110Pro)	c.329T>C	rs11466018	0.006366	0.08509	0.0001265	Uncertain significance (VUS)/VALIDATED	Common variants often allelic (complex alleles)
E148Q	2		p.(Glu148Gln)	c.442G>C	rs3743930	0.06576	0.2915	0.01353	Uncertain significance (VUS)/VALIDATED	Common variants often allelic (complex alleles)
E167D	2		p.(Glu167Asp)	c.501G>C	rs104895079	0.00004693	0.000	0.00009827	Likely pathogenic/PROVISIONAL	
R202Q	2		p.(Arg202Gln)	c.605G>A	rs224222	0.2354	0.04334	0.2736	Benign/VALIDATED	
S208C	2		p.(Ser208Cys)	c.622A>T					Uncertain significance (VUS)/PROVISIONAL	
S208T	2		p.(Ser208Thr)	c.623G>C	rs759326778	0.00003772	0.000	0.000	Likely pathogenic/To be validated	
S242R	2		p.(Ser242Arg)	c.726C>G	rs104895127	0.000003980	0.000	0.000	Likely pathogenic/VALIDATED	Dominant inheritance (PAAND)
E244K	2		p.(Glu244Lys)	c.730G>A					Not classified/To be validated	Dominant inheritance (PAAND)
P257L	2		p.(Pro257Leu)	c.770C>T	rs201025181	0.000003977	0.00005437	0.000	Uncertain significance (VUS)/To be validated	
T267I	2	bZIP	p.(Thr267Ile)	c.800C>T	rs104895081	0.0001485	0.000	0.0001703	Likely pathogenic/VALIDATED	
G304R	2		p.(Gly304Arg)	c.910G>A	rs75977701	0.004685	0.01806	0.001017	Likely benign/VALIDATED	
P369S	3		p.(Pro369Ser)	c.1105C>T	rs11466023	0.01470	0.07148	0.009158	Uncertain significance (VUS)/VALIDATED	Common variants often allelic (complex alleles)
P373L	3	Bbox	p.(Pro373Leu)	c.1118C>T					Uncertain significance (VUS)/VALIDATED	Dominant inheritance (FMF-like)
R408Q	3	Bbox	p.(Arg408Gln)	c.1223G>A	rs11466024	0.01336	0.05378	0.009130	Uncertain significance (VUS)/PROVISIONAL	Common variants often allelic (complex alleles)
H478Y	5		p.(His478Tyr)	c.1432C>T	rs104895105				Uncertain significance (VUS)/VALIDATED	Dominant inheritance (FMF-like)
F479L	5		p.(Phe479Leu)	c.1437C>G	rs104895083	0.00004242	0.000	0.00009288	Likely pathogenic/VALIDATED	
S503C	5		p.(Ser503Cys)	c.1508C>G	rs190705322	0.00007555	0.0009786	0.000	Likely pathogenic/VALIDATED	
T577A	8		p.(Thr577Ala)	c.1729A>G					Likely pathogenic/PROVISIONAL	Dominant inheritance (FMF-like)
T577N	8		p.(Thr577Asn)	c.1730C>A	rs1057516210				Likely pathogenic/VALIDATED	Dominant inheritance (FMF-like)
T577S	8		p.(Thr577Ser)	c.1729A>T	rs104895193				Likely pathogenic/PROVISIONAL	Dominant inheritance (FMF-like)
I591T	9		p.(Ile591Thr)	c.1772T>C	rs11466045	0.01089	0.00005015	0.01650	Uncertain significance (VUS)/PROVISIONAL	Common variants often allelic (complex alleles)
N679H	10	B30.2	p.(Asn679His)	c.2035A>C					Not classified/To be validated	

M680I	10	B30.2	p.(Met680Ile)	c.2040G>A	rs28940580	0.000007953	0.000	0.00001758	Pathogenic/VALIDATED	Classical FMF (criteria and ethnicity)
I692del	10	B30.2	p.(Ile692del)	c.2076_2078del	rs104895093	0.000007953	0.000	0.000008790	Likely pathogenic/VALIDATED	
M694I	10	B30.2	p.(Met694Ile)	c.2082G>A	rs28940578	0.0001273	0.000	0.0001471	Pathogenic/VALIDATED	Classical FMF (criteria and ethnicity)
M694V	10	B30.2	p.(Met694Val)	c.2080A>G	rs61752717	0.0002722	0.000	0.0004567	Pathogenic/VALIDATED	Classical FMF (criteria and ethnicity)
M694del	10	B30.2	p.(Met694del)	c.2081_2083del	rs104895091	0.000007953	0.000	0.00001758	Likely pathogenic/VALIDATED	Sometimes associated with dominant transmission
K695R	10	B30.2	p.(Lys695Arg)	c.2084A>G	rs104895094	0.005826	0.000	0.007942	Likely pathogenic/VALIDATED	
V726A	10	B30.2	p.(Val726Ala)	c.2177T>C	rs28940579	0.001983	0.000	0.0008902	Pathogenic/VALIDATED	Classical FMF (criteria and ethnicity)
A744S	10	B30.2	p.(Ala744Ser)	c.2230G>T	rs61732874	0.001764	0.000	0.001603	Uncertain significance (VUS)/VALIDATED	
R761H	10	B30.2	p.(Arg761His)	c.2282G>A	rs104895097	0.0002051	0.001904	0.00007743	Likely pathogenic/VALIDATED	
6 combined variants										

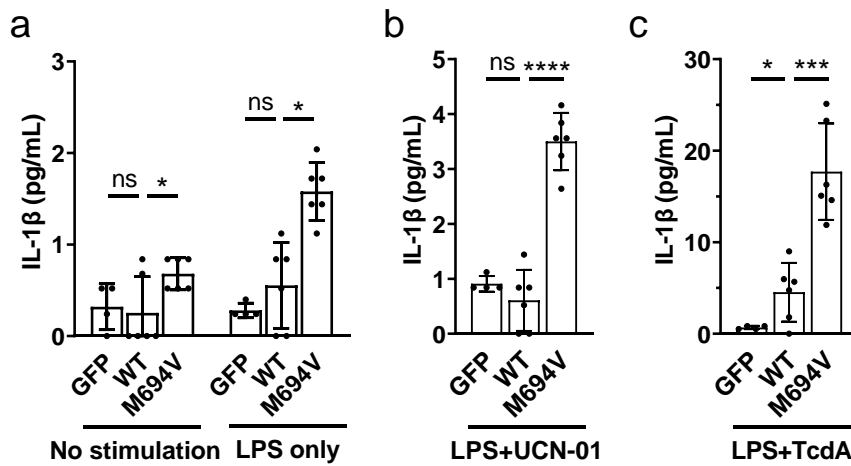
6 combined variants: *MEFV*^{L110P-E148Q-R202Q-P369S-R408Q-S503}; PYD: pyrin domain; VUS: variants of unknown significance; PAAND: pyrin-associated autoinflammation with neutrophilic dermatosis; FMF: Familial Mediterranean fever

Figure S1 7-AAD/Annexin V staining in GFP-positive cells



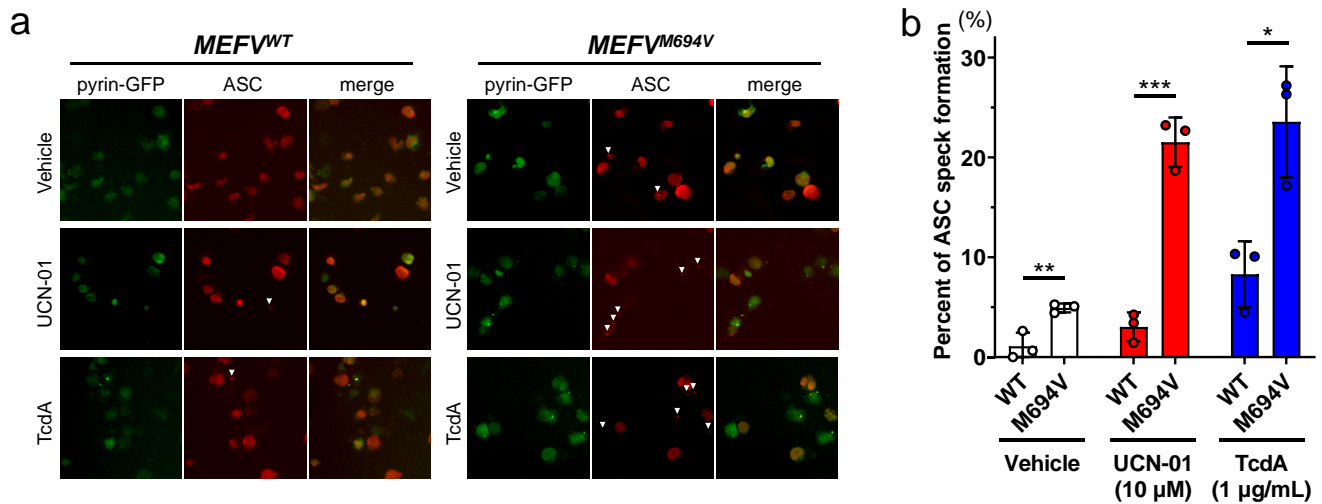
(a) Representative flow-cytometry dot plots by 7-AAD and Annexin V staining among GFP-positive cells. The number in each quadrant indicates the percentage of the cells. Blue rectangles indicate 7-AAD-negative and Annexin V-positive cells (early apoptosis). The percentage of cells (b) in each quadrant and (c) in 7-AAD-negative/Annexin V-positive among GFP-positive population. Cells were stimulated 3 h after transfection and analyzed by flow-cytometry 6 h after nucleofection. Data were analyzed by unpaired two-tailed t-test. ns: nonsignificant, * $p < 0.05$, ** $p < 0.01$, *** $p < 0.001$, **** $p < 0.0001$. Data represent the mean \pm standard deviation of three independent assays

Figure S2 IL-1 β production from transfected THP-1 cells



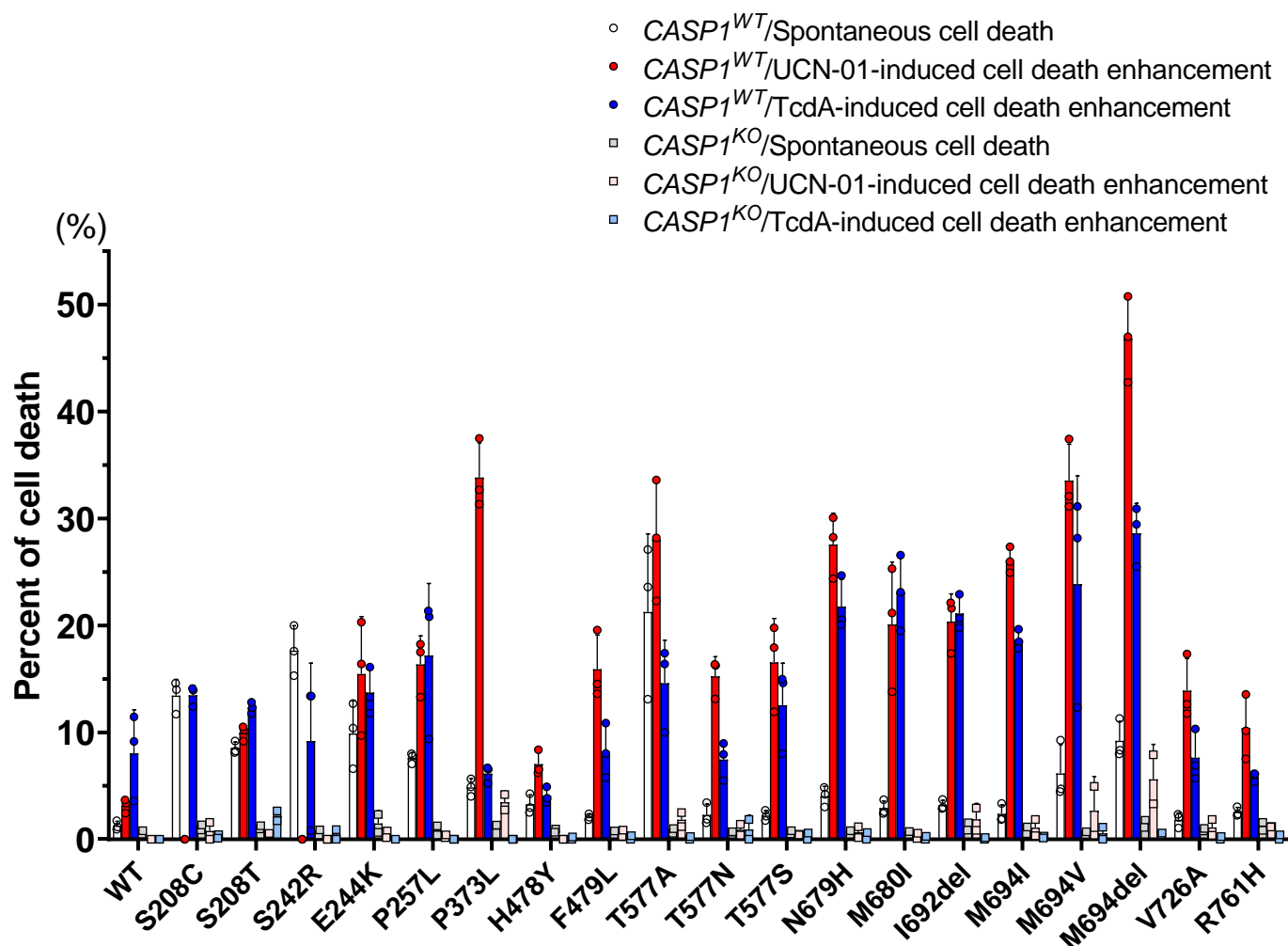
Cells were primed with LPS (100 ng/mL) immediately after nucleofection for 3 hours when indicated. After 3 hours of nucleofection, cells were (a) left untreated (no stimulation and LPS-primed only), stimulated with (b) UCN-01 (10 μ M), or (c) TcdA (1 μ g/mL) for additional 3 hours. Supernatant was collected 6 h after nucleofection and analyzed for IL-1 β . Data were analyzed by unpaired two-tailed t-test. ns: nonsignificant, * p < 0.05, ** p < 0.01, *** p < 0.001, **** p < 0.0001. Data represent the mean \pm standard deviation of three independent assays

Figure S3 ASC speck formation in transfected THP-1 cells



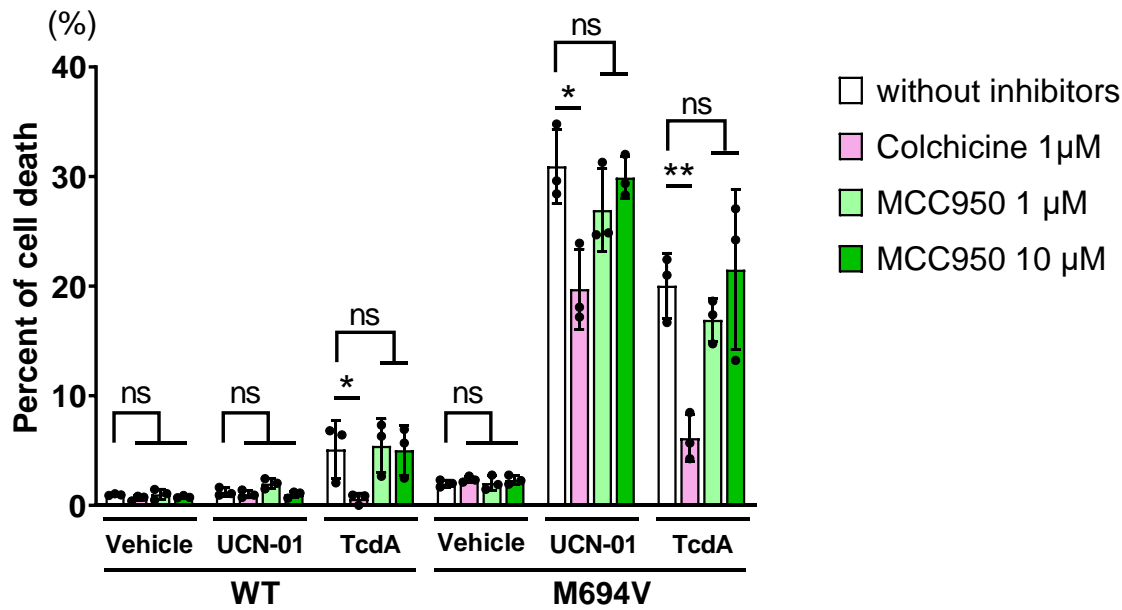
(a) Representative fluorescence microscopy images for quantifying ASC speck formation in THP-1 cells transfected with GFP-fused *MEFV^{WT}* (left) or *MEFV^{M694V}* (right); top: no-stimulation, middle: UCN-01 stimulation, bottom: TcdA stimulation. **(b)** Quantification of ASC speck formation. Cells were stimulated 3 h after transfection and fixed for analysis 6 h after nucleofection. Data were analyzed by unpaired two-tailed t-test. ns: nonsignificant, * $p < 0.05$, ** $p < 0.01$, *** $p < 0.001$, **** $p < 0.0001$. Data represent the mean \pm standard deviation of three independent assays

Figure S4 Cell death by each *MEFV* variant was prevented by caspase-1 knockout.



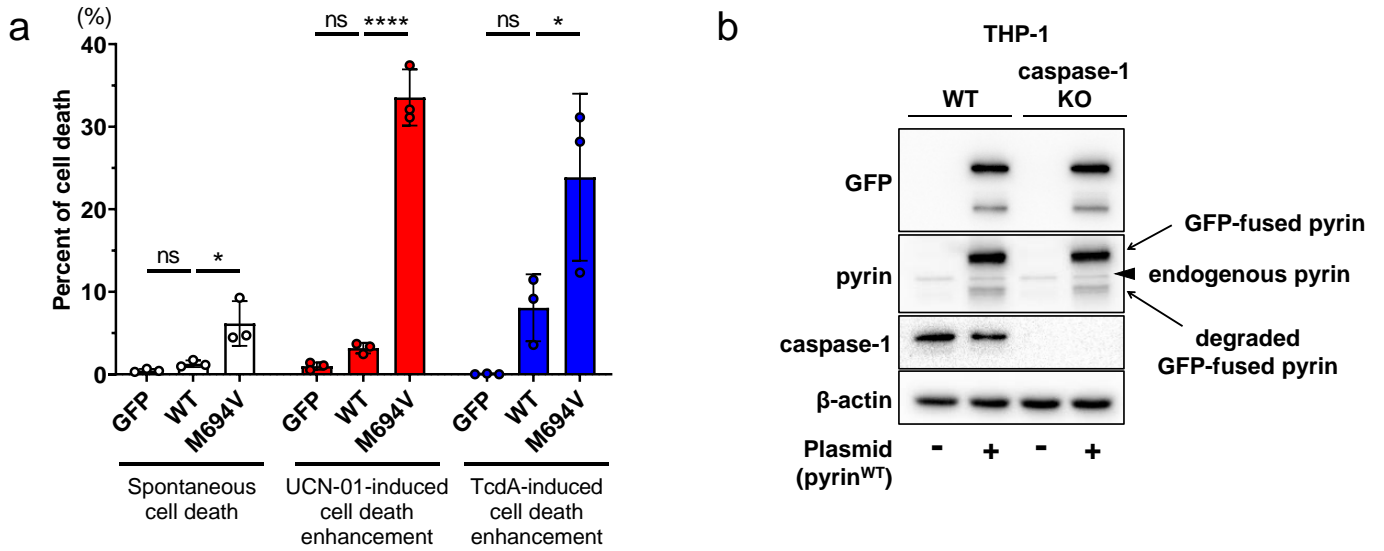
Cells were stimulated 3 h after transfection and fixed for analysis 6 h after nucleofection. Cell death was calculated as the percentage of 7-AAD-positive cells among GFP-positive cells. Circle: *CASP1*^{WT} THP-1, rectangle: *CASP1*^{KO} THP-1. White/gray: spontaneous cell death; red/pink: UCN-01-induced cell death enhancement; blue/light blue: TcdA-induced cell death enhancement. Spontaneous cell death indicates cell death without stimulation. UCN-01/TcdA-induced cell death enhancement was defined as the increased percentage of cell death upon UCN-01/TcdA stimulation over spontaneous cell death: ((percentage of cell death upon UCN-01/TcdA stimulation) - (percentage of spontaneous cell death)). If UCN-01/TcdA-induced cell death enhancement was a negative value, 0 was plotted. Data represent the mean ± standard deviation of three (for *CASP1*^{WT} THP-1) or two (for *CASP1*^{KO} THP-1) independent assays

Figure S5 Cell death was inhibited by colchicine but not by MCC950.



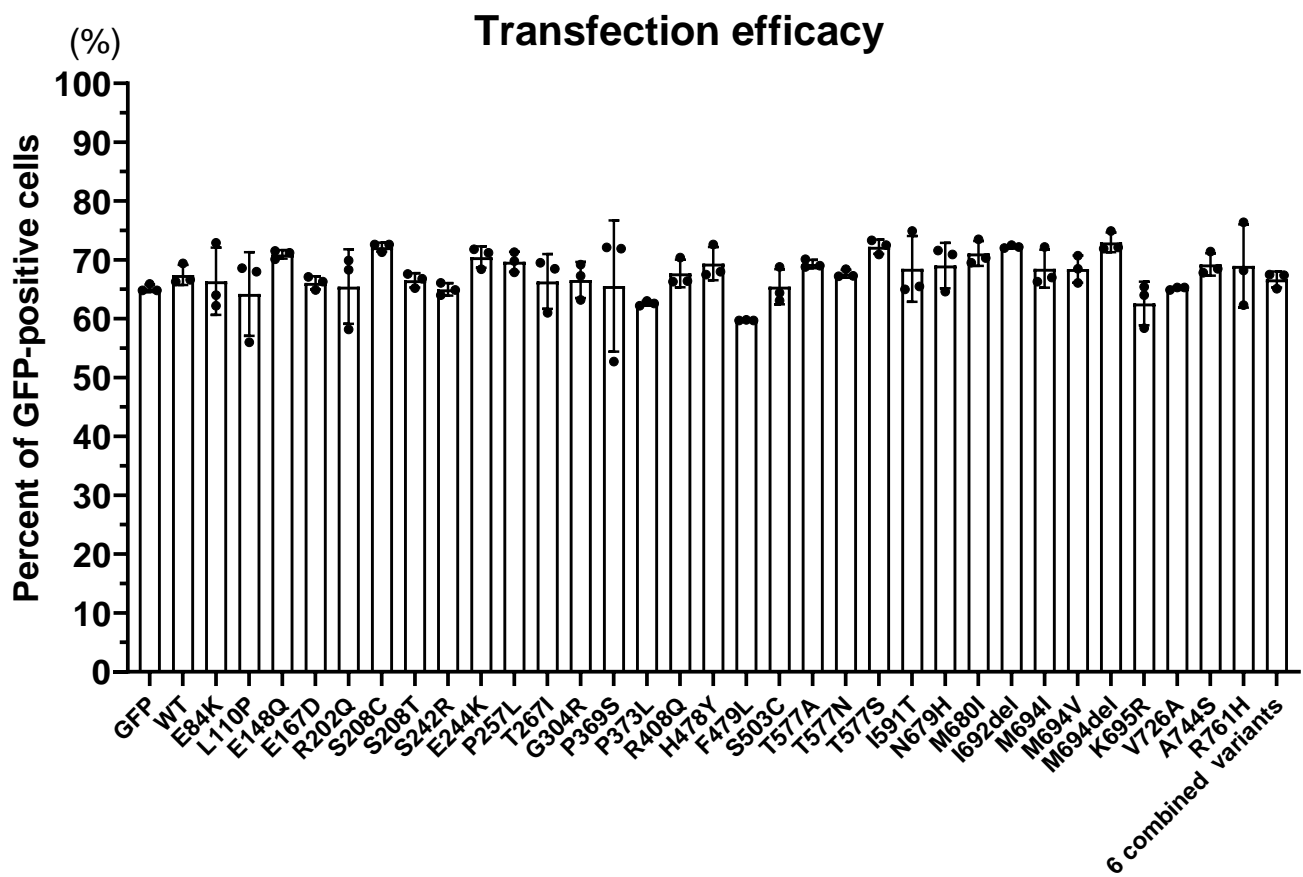
Quantification of cell death (spontaneous cell death and UCN-01/TcdA-induced cell death enhancement) caused by each *MEFV* variant. Colchicine (1 μM) or MCC950 (1 or 10 μM) was added 2 hours after nucleofection. Three hours after nucleofection, cells were stimulated with UCN-01 (10 μM)/TcdA (1 μg/mL) for additional 3 hours and analyzed by flow cytometry. Cell death was calculated as the percentage of 7-AAD-positive cells among GFP-positive cells. Spontaneous cell death indicates cell death without stimulation. UCN-01/TcdA-induced cell death enhancement was defined as the increased percentage of cell death upon UCN-01/TcdA stimulation over spontaneous cell death: ((percentage of cell death upon UCN-01/TcdA stimulation) - (percentage of spontaneous cell death)). If UCN-01/TcdA-induced cell death enhancement was a negative value, 0 was plotted. Data were analyzed by unpaired two-tailed t-test. ns: nonsignificant, * $p < 0.05$, ** $p < 0.01$, *** $p < 0.001$, **** $p < 0.0001$. Data represent the mean \pm standard deviation of three independent assays

Figure S6 Endogenous pyrin expression was almost negligible in this assay.



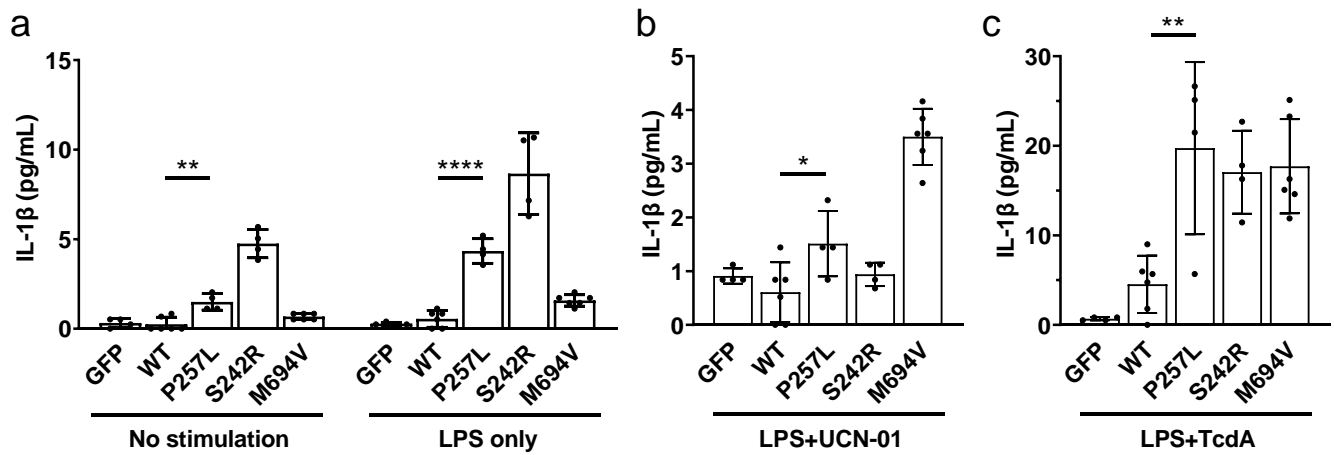
(a) Quantification of cell death caused by each *MEFV* variant. Three hours after nucleofection, cells were left untreated or stimulated with UCN-01 (10 μ M)/TcdA (1 μ g/mL) for additional 3 hours, and analyzed by flow cytometry. Cell death was calculated as the percentage of 7-AAD-positive cells among GFP-positive cells. Spontaneous cell death (white) indicates cell death without stimulation. UCN-01 (red)/TcdA (blue)-induced cell death enhancement was defined as the increased percentage of cell death upon UCN-01/TcdA stimulation over spontaneous cell death: ((percentage of cell death upon UCN-01/TcdA stimulation) - (percentage of spontaneous cell death)). If UCN-01/TcdA-induced cell death enhancement was a negative value, 0 was plotted. Data were analyzed by one-way ANOVA followed by Dunnett's multiple comparison test (versus the WT as a control group). ns: nonsignificant, * $p < 0.05$, ** $p < 0.01$, *** $p < 0.001$, **** $p < 0.0001$. Data represent the mean \pm standard deviation of three independent assays. **(b)** Western blot of *CASP1*^{WT}/*CASP1*^{KO} THP-1 with or without GFP-fused *MEFV*^{WT} transfection. *MEFV* overexpression was detected using anti-GFP antibodies. Endogenous (arrowhead) and overexpressed *MEFV* (arrow) were both detected using anti-pyrin antibodies

Figure S7 Transfection efficiency assessed by GFP expression



The percentages of GFP-positive cells per transfection were measured. Cells were analyzed 6 h after nucleofection. Data represent the mean \pm standard deviation of three independent assays. 6 combined variants: *MEFV*^{L110P-E148Q-R202Q-P369S-R408Q-S503}

Figure S8 IL-1 β production from THP-1 cells transfected with *MEFV*^{P257L}



Cells were primed with LPS (100 ng/mL) immediately after nucleofection for 3 hours when indicated. After 3 hours of nucleofection, cells were (a) left untreated (no stimulation and LPS-primed only), stimulated with (b) UCN-01 (10 μ M), or (c) TcdA (1 μ g/mL) for additional 3 hours. Culture supernatants were collected 6 h after nucleofection and analyzed for IL-1 β . Data were analyzed by unpaired two-tailed t-test. ns: nonsignificant, * $p < 0.05$, ** $p < 0.01$, *** $p < 0.001$, **** $p < 0.0001$. Data represent the mean \pm standard deviation of three independent assays